Spectroscopy of Heavy Quarkonia and Fine and Hyperfine Structures

森下, 淳也

(Degree)
博士（学術）

(Date of Degree)
1984-03-31

(Date of Publication)
2007-10-11

(Resource Type)
doctoral thesis

(Report Number)
甲0464

(URL)
https://hdl.handle.net/20.500.14094/D1000464

December 1983

Spectroscopy of Heavy Quarkonia and Fine and Hyperfine Structures

重クォーコニウムの分光学と微細及び超微細構造

Jun-ya Morishita

Department of Information and Instrumentation
Division of System Science
Graduate School of Science and Technology
Kobe University

ACKNOWLEDGMENTS

I would like to express my gratitude to Professor Masaaki Kawaguchi for his stimulating suggestions and discussions concerning this thesis and for his generous guidance and encouragement during all of my course at this graduate school.

I owe many thanks to Professor Tetsuro Kitazoe, Professor Makoto Kaburagi, Dr. Makoto Oka and Dr. Hiroshi Munakata for their valuable suggestions and discussions and for leading me to finish this work as coworkers. They readily agreed to publication of this work for my doctoral thesis.

I am grateful to Professor Toshiyuki Morii, Professor Taizo Muta, Dr. Jiro Kodaira and Mr. Mitsutoshi Wada for their useful discussions.

I would like to thank the members of National Laboratory for High Energy Physics (KEK) for the kind hospitality during my second grade.

Numerical calculation was almost performed by the ACOS 900/1000 (NEC) computer at the Computer Center, Kobe University and was supported in part by the Institute for Nuclear Study, University of Tokyo.

This script was typed by the ACOS 1000 computer using word processor routine in FORTRAN written by Professor Atsuo Ono.

ABSTRACT

We study spectroscopies of the heavy quarkonia, $c\bar{c}$, $b\bar{b}$ and $t\bar{t}$ in the framework of the nonrelativistic potential model. Relativistic corrections are taken into account up to the order of $(p/m)^2$. Spin dependent interactions which cause the fine and hyperfine splittings are investigated in detail. It is pointed out that the naive linear plus Coulomb model cannot explain both the fine and hyperfine splittings consistently, due to the strong spin-spin force coming from the Coulomb potential. We propose a flavor independent potential which has a Lorentz vector term determined by perturbative quantum chromodynamics (QCD) at short distances and connected to the Coulomb potential at large distances. It is emphasized that this short range attenuation of the vector Coulomb potential has a remarkable effect on the hyperfine structure of the $c\bar{c}$ and $b\bar{b}$ systems. The hyperfine splitting between $^3S_1$ and $^1S_0$ in the charmonium are well recovered by this modification and resulting spectra of the $c\bar{c}$ and $b\bar{b}$ excellently agree with experiment. It is also found that the short range attenuation plays an important role in the $t\bar{t}$ level structure. We study the decay properties of the heavy quarkonia using calculated wave functions. We discuss the scale parameter Λ obtained from the potential with perturbative QCD as compared with that obtained from the Υ decays.

CONTENTS

1. INTRODUCTION

Heavy quarkonia $c\bar{c}$, $b\bar{b}$ and $t\bar{t}$ are very nice objects to investigate hadronic structure. Experimentally they show strong narrow resonances so that we can get precise data on mass spectra. It is expected that their flavor mixings are negligible and their theoretical treatment is easy. As a future problem investigation of the topponium $t\bar{t}$ is the most fascinating topics of particle physics. The top quark is a partner of the b quark doublet which we have not yet found. Many experiments have been done and prepared for the purpose of detecting it. First candidate was obtained from data analysis of $p\bar{p}$ colliding beam experiment at CERN[1] and resulting mass of the top quark is about 35 GeV. In this energy region some e^+e^- experiments are planned to detect the first signal of the topponium $t\bar{t}$, for example, by TRISTAN at KEK.[2] Anyway it is important to examine characteristic properties of the topponium spectra as precise as possible, which would help us in both experimental observation and theoretical analysis.

Nonrelativistic potential model is the most popular and powerful tool to study spectra of bound states. Detailed observations of heavy quarkonium spectroscopy in the $c\bar{c}$ and $b\bar{b}$ systems have led us to obtain a unified view of the potential between a heavy quark and its antiquark.[3 - 5] Almost all the potentials which have been proposed so far as to describe these systems agree in the intermediate range $0.5\ \mathrm{GeV}^{-1} \lesssim r \lesssim 5\ \mathrm{GeV}^{-1}$, where these ground states have average radii. The spectroscopy of the heavy quarkonia is in a situation similar to that which we met in the atomic physics almost half a century ago. We have quantum chromodynamics (QCD) in the quarkonium physics instead of the quantum electrodynamics (QED) in the atomic physics. There

exists, however, an essential differece between QCD and QED. While QED is well governed by the perturbative nature, QCD has nonperturbative phenomena in addition to the perturbative one. The heavy quarkonium system is an ideal place to study and test QCD because the potential is under the influence of both perturbative and nonperturbative phenomena.

The purpose of this paper is to determine the $Q\bar{Q}$ potential most accurately by studying the $c\bar{c}$ and $b\bar{b}$ spectroscopy and to apply it to the topponium $t\bar{t}$. The success of potential models established so far is enough to predict the spectra of the center of gravity (c.o.g.), where c.o.g. is defined as a degenerate level when the spin dependent interactions are switched off. Here our interest is how to understand fine and hyperfine structures in the heavy quarkonium spectroscopy.[6 - 8] Relativistic corrections are taken into account as much as possible in order to investigate the fine and hyperfine splittings in the heavy quarkonia.

In studying fine and hyperfine structures, the Lorentz transformation properties of the potential become a serious problem. There are much difference in the spin dependence of hamiltonian whether the static potentials are transformed as a scalar or the fourth component of a vector. It is well known that any pure vector potential cannot explain the splittings of the charmonium ^3P states.[9] From investigation of the Dirac hamiltonian it is also suggested that the confining potential should be a scalar in order to avoid the Klein paradox.[10,11] Among several potentials, we think it reasonable to take potentials of the confinement plus Coulomb type proposed by Cornell group[3] as a prototype. Consequently we assume that the confining potential has a scalar coupling to a quark and the Coulomb potential has a vector one.

The perturbative QCD corrections, which we have not yet included the above assumptions, must be taken into account. Actually our prototype can not reproduce experimental data, as is shown in Section 3. The relativistic effects to cause fine and hyperfine splittings are almost determined the behavior of the potential at short distances where the perturbative QCD plays an important role. Buchmüller and Tye[12] employed a hybrid model which incorporates the perturbative QCD at short distances and a linear confinement at large distances. They assumed that the perturbative term is connected to the confining part according to the idea of Richardson[13] and that the scale parameter Λ in the potential is determined by smooth connection of the perturbative QCD form at short distances with the linear confining potential. However their range connected potentials is very small, $r < 0.05$ GeV^{-1} and this potential does not approach the perturbative QCD form yet in the asymptotic free region $r \lesssim 0.3$ GeV^{-1}.

We take another way to incorporate the perturbative QCD and the $Q\bar{Q}$ potential. We assume that the perturbative form in the asymptotic free region is continuously connected to a vector Coulomb one in long range. The confining potential is assumed as a scalar and vanishes at the perturbative region ($r \lesssim 0.5$ GeV^{-1}) so that the whole potential fits well to the perturbative QCD at short distances. Λ parameter is given by comparing the fine and hyperfine structures of $c\bar{c}$ and $b\bar{b}$ systems with experiment. Thus we will establish an overall fitting of $c\bar{c}$ and $b\bar{b}$ spectra.

This paper is organized as follows. In Section 2, the hamiltonian with a scalar plus vector potential is constructed and the general properties of the spin dependent forces are discussed, which cause the fine and hyperfine splittings. It is also indicated that the spin independent corrections up to the order $(p/m)^2$ are important as well as the spin dependent

corrections. Section 3 is devoted to show that the naive linear plus Coulomb model cannot give a consistent description of the fine and hyperfine splittings of the charmonium. It is suggested that the difficulties are mainly coming from the short range behavior of the vector potential. We propose in Section 4 a model with a modified vector potential according to the idea mentioned above. In Section 5 we apply this model to the spectra of heavy quarkonia. Parameters are determined so as to fit the observed levels of ψ and Υ families and the spectrum of the $t\bar{t}$ is predicted by using this potential. The scale parameter Λ is determined as 0.36 GeV from the best fitting to the data. In Section 6 decays of heavy quarkonia are investigated. The annihilation widths of Υ decays are found to be much improved compared with the naive linear plus Coulomb model. Decays of $t\bar{t}$ are also predicted and discussed. Section 7 is devoted to summary and discussions.

2. HAMILTONIAN OF THE HEAVY QUARKONIUM

Relativistic corrections to the nonrelativistic hamiltonian are derived from the Bethe-Salpeter (BS) equation by the Foldy-Wouthuysen (FW) transform:[14] The instantaneous approximation of the BS equation is taken and the resulting equation is expanded by $(p/m)^2$. Here the expansion is carried out up to the order of $(p/m)^2$ explicitly. Next order corrections of the order $(p/m)^4$ to energy levels are expected a few MeV for the $c\bar{c}$ and $b\bar{b}$ systems. For the $t\bar{t}$ system they become even smaller. In the present case instantaneous interaction in the BS equation is a combination of a Lorentz scalar S(r) and a vector V(r). The vector potential has a transverse component as well as a longitudinal one. We call hereafter the relativistic corrections of the order $(p/m)^2$ Breit-Fermi (BF) interaction according to the similarity to the original Breit-Fermi interaction appeared in QED.

Thus the hamiltonian of the quark-antiquark system ($Q\bar{Q}$) is given as follows[14,15]:

$$H = H_0 + T_{p4} + H_{BF}, \tag{2-1}$$

with

$$H_0 = 2m_Q + \frac{p^2}{m_Q} + S(r) + V(r), \tag{2-2}$$

$$T_{p4} = -\frac{p^4}{4m_Q^3}, \tag{2-3}$$

and

$$H_{BF} = H_{BF}^{S} + H_{BF}^{V}, \tag{2-4}$$

where $\vec{p}$ is the relative momentum between the quark and the antiquark and m_Q is the quark mass. The BF interaction consists of two parts, H_{BF}^{V} and H_{BF}^{S}. The H_{BF}^{V} is originated to the vector potential V(r) and is given by

$$H_{BF}^{V} = V_{SI} + V_{SS} + V_{LS} + V_{T}, \tag{2-5}$$

where

$$V_{SI} = -\frac{1}{m_Q^2}\left(\frac{1}{4}\Delta V + VP^2 - f(U_V)\right), \quad \text{(spin-independent term)} \tag{2-6}$$

$$V_{SS} = \frac{1}{6m_Q^2}(\vec{\sigma}_1\vec{\sigma}_2)\Delta V, \quad \text{(spin-spin term)} \tag{2-7}$$

$$V_{LS} = \frac{3}{4m_Q^2}(\vec{\sigma}_1 + \vec{\sigma}_2)\cdot\vec{L}\frac{1}{r}\frac{dV}{dr}, \quad \text{(spin-orbit term)} \tag{2-8}$$

and

$$V_T = -\frac{1}{12m_Q^2}S_{12}\left(\frac{d^2V}{dr^2} - \frac{1}{r}\frac{dV}{dr}\right). \quad \text{(tensor term)} \tag{2-9}$$

Here $\vec{\sigma}_i$ denotes the Pauli spin operator of the i-th quark, $\vec{L}$ is the relative orbital angular momentum and $\vec{P} = (\overleftarrow{\nabla} + \vec{\nabla})/2i$ is defined as the average momentum of the initial and final relative ones. The tensor operator S_{12} is defined by

$$S_{12} = 3(\vec{\sigma}_1\vec{n})(\vec{\sigma}_2\vec{n}) - (\vec{\sigma}_1\vec{\sigma}_2), \tag{2-10}$$

where $\vec{n} = \vec{r}/|\vec{r}|$, a unit vector pointed to the direction of the relative coordinate. The H_{BF}^{S} comes from the scalar potential and

is written by

$$H_{BF}^{S} = S_{SI} + S_{LS}, \tag{2-11}$$

with

$$S_{SI} = -\frac{1}{m_Q^2}(SP^2 - f(U_S)), \qquad \text{(spin-independent term)} \tag{2-12}$$

and

$$S_{LS} = \frac{1}{4m_Q^2}(\vec{\sigma}_1 + \vec{\sigma}_2)\cdot\vec{L}\,\frac{1}{r}\frac{dS}{dr}. \qquad \text{(spin-orbit term)} \tag{2-13}$$

Retardation effects are approximately taken into account according to a prescription of Gromes',[14] which reproduce the original BF potential in case of the vector Coulomb potential. His method is available in case of other Lorentz type of various potentials. They are given in the last terms of eqs. (2-6) and (2-12), where

$$f(U) = P^2\frac{1}{r}\frac{dU}{dr} + (\vec{P}\cdot\vec{n})^2\left(\frac{d^2U}{dr^2} - \frac{1}{r}\frac{dU}{dr}\right), \tag{2-14}$$

with the solutions of

$$\nabla^2 U_V = \frac{1}{2}\vec{\nabla}\cdot\vec{r}V(r), \tag{2-15}$$

and

$$\nabla^2 U_S = \frac{1}{2}\vec{\nabla}\cdot\vec{r}S(r), \tag{2-16}$$

It should be noted that some objections to the Gromes' treatment for the retardation effects of the scalar potential are raised by some authors[16,17], who pointed out that his treatment does not

satisfy a criterion which in the limit that one of two quarks has an infinite mass the above procedure of the BS equation is consistent with the FW transform of the Dirac equation in an external source. However what the correct approximation of the scalar retardation effects must be is still an open problem. Here the Gromes' treatment is assumed for the scalar retardation effects.

The Schrödinger equation for H_0, eq.(2-2),

$$H_0\Psi(\vec{r}) = E\Psi(\vec{r}), \tag{2-17}$$

is solved by the variational method and the other terms T_{p4} and H_{BF} are taken into account by the first order perturbation. Wave function $\Psi(\vec{r})$ in the spherical coordinate can be separated as

$$\Psi(\vec{r}) = R(r)Y_{LM}(\vec{\Omega}), \tag{2-18}$$

where $R(r) = w(r)/r$ and $Y_{LM}(\vec{\Omega})$ is the spherical harmonics. We take a trial function of $w(r)$ which depends on a number of parameters and vary these parameters to minimize the eigenvalue E. Spin singlet and triplet states are degenerate in the unperturbed H_0 and are splitted by the spin-spin term eq.(2-7) (hyperfine splitting). Different J (total angular momentum) levels of the spin triplet state are also degenerate in H_0 and splitted by the spin-orbit terms, eqs.(2-8) and (2-13), and by the tensor term, eq.(2-9) in H_{BF}. Mixings of different L states such as $^3S_1$ and $^3D_1$ take place due to the tensor term, eq.(2-9), which are neglected here because they are not important so far as the energy levels of heavy quarkonia are concerned. The T_{p4} of eq.(2-3) and the spin independent terms, V_{SI} of eq.(2-6) and S_{SI} of eq.(2-12), which give shifts of c.o.g.'s, are significant in

the quarkonium spectra as shown in Section 5. The explicit forms of the differential and spin-dependent operators appeared in this section are given in Appendix A in order to help the discussions.

The relation between the BF interaction and the higher order corrections in the perturbative QCD was discussed by Schnitzer.[6] He showed that the former coincides with the latter except for some singular terms of $\ln(Q^2/m^2)$ dependence. A rough estimation is made for these singular terms in Section 7.

3. DIFFICULTIES IN "LINEAR PLUS COULOMB" POTENTIAL

It is well known that the experimental value ~ 0.5 of the ratio for the charmonium 1P states,

$$R = [M(^3P_2)-M(^3P_1)]/[M(^3P_1)-M(^3P_0)], \tag{3-1}$$

cannot be reproduced with the spin-orbit and the tensor terms coming from the pure vector potential.[10] To see this let us consider the vector linear plus Coulomb potential. From the Coulomb potential, the spin-orbit term of eq.(2-8) gives $R = 2$ due to the coefficient $\vec{\sigma}\cdot\vec{L}$ (See Table 5) and the tensor term reduces this down to $R = 0.8$. Adding the effect of vector linear potential the spin-orbit strength becomes larger and also enlarges the ratio but the tensor force cannot contribute so enough to reduce the ratio as the Coulomb potential does, then the resulting ratio is at most $R \simeq 1.0$. This result is in contradiction with experiment. The BF interaction coming from the scalar confining potential remedies this difficulty; it reduces the strength of the spin-orbit terms but does not contribute to the tensor force at all.

Next, let us consider the "Linear plus Coulomb" model with the scalar confining potential,

$$S(r) = -\frac{r}{a^2} + b, \tag{3-2}$$

and the vector Coulomb potential,

$$V(r) = -\frac{4}{3}\frac{\alpha_s}{r}. \tag{3-3}$$

It is well known that this model can explain the gross structures

of the charmonium and bottomonium spectra.[3] Unfortunately it will be pointed out below that this model can reproduce either the S state hyperfine splitting or the P state fine splitting in the charmonium spectra but cannot both at the same time.

First, consider a potential which reproduces the $^3S_1$ and $^1S_0$ states of the charmonium where parameters a, b, α_s, m_c and m_b are determined so as to fit the levels J/ψ, η_c, ψ', η_c', Υ and Υ'. Figure 1a shows the resulting $c\bar{c}$ and $b\bar{b}$ spectra. It is seen that the magnitude of the 1P's fine splitting becomes too small compared with experiment. Next, consider another potential which reproduces the 1P states of the charmonium, where parameters a, b, α_s and m_c are determined so as to fit the levels of χ state, the c.o.g.'s of J/ψ and η_c and that of ψ' and η_c'. The resulting spectra are given in Fiure 1b and shows the hyperfine splittings $J/\psi - \eta_c$ and $\psi' - \eta_c'$ become too large and almost twice as much as the experimental values. These lead us to conclusion that the linear plus Coulomb potential model cannot explain both the hyperfine splitting ($^3S_1 - {}^1S_0$) and the fine splitting ($^3P_2 - {}^3P_1 - {}^3P_0$) consistently. Thus the naive linear plus Coulomb model must be modified to reproduce the fine and hyperfine structures of the quarkonium spectra. When one adopts modification, there are two ways to remedy the difficulties. One is that the difficuties are mainly in the fine splitting and it should be corrected by appropriate modification, and another is that the hyperfine splitting should be changed to improve the potential. The former approach has been taken by many authors and led us many ideas such as an introduction of the color anomalous magnetic moment of a quark.[18,19] This modification affects only the splittings of 1P states and not change the c.o.g!s of them. We must, however, raise up their c.o.g!s by appropriate modification. (See Figure 1a.) Therefore we adopt here the latter

approach and suggest that the too large hyperfine splitting makes us difficult to explain the quarkonium spectra.

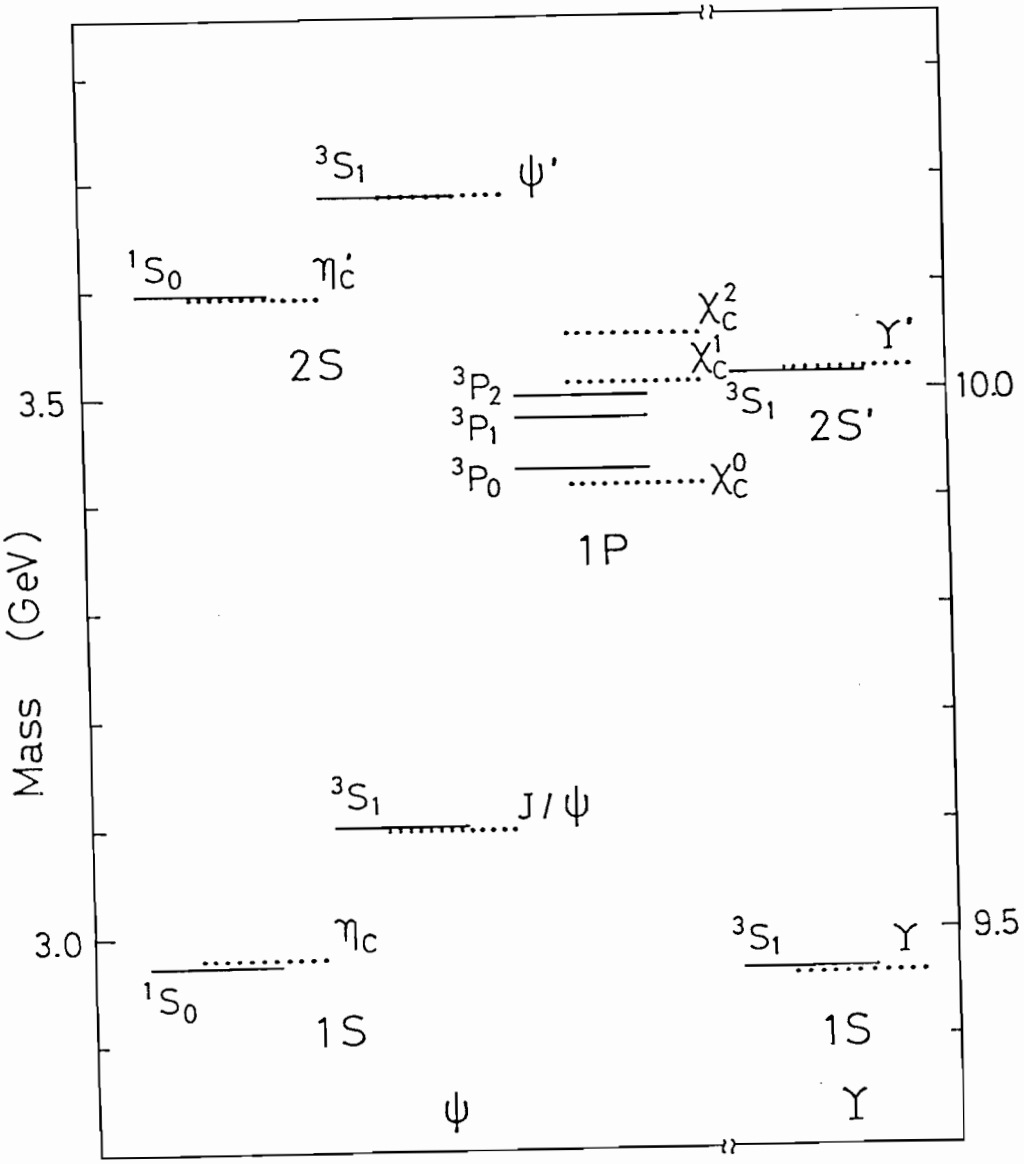

Fig. 1a. Spectra in the linear plus Coulomb model which reproduce the hyperfine splitting. Parameters are a = 1.632 GeV^{-1}, b = -0.5466 GeV, α_s = 0.3548, m_c = 1.632 GeV and m_b = 5.015 GeV. The dotted lines are exprimental data taken from reference (20).

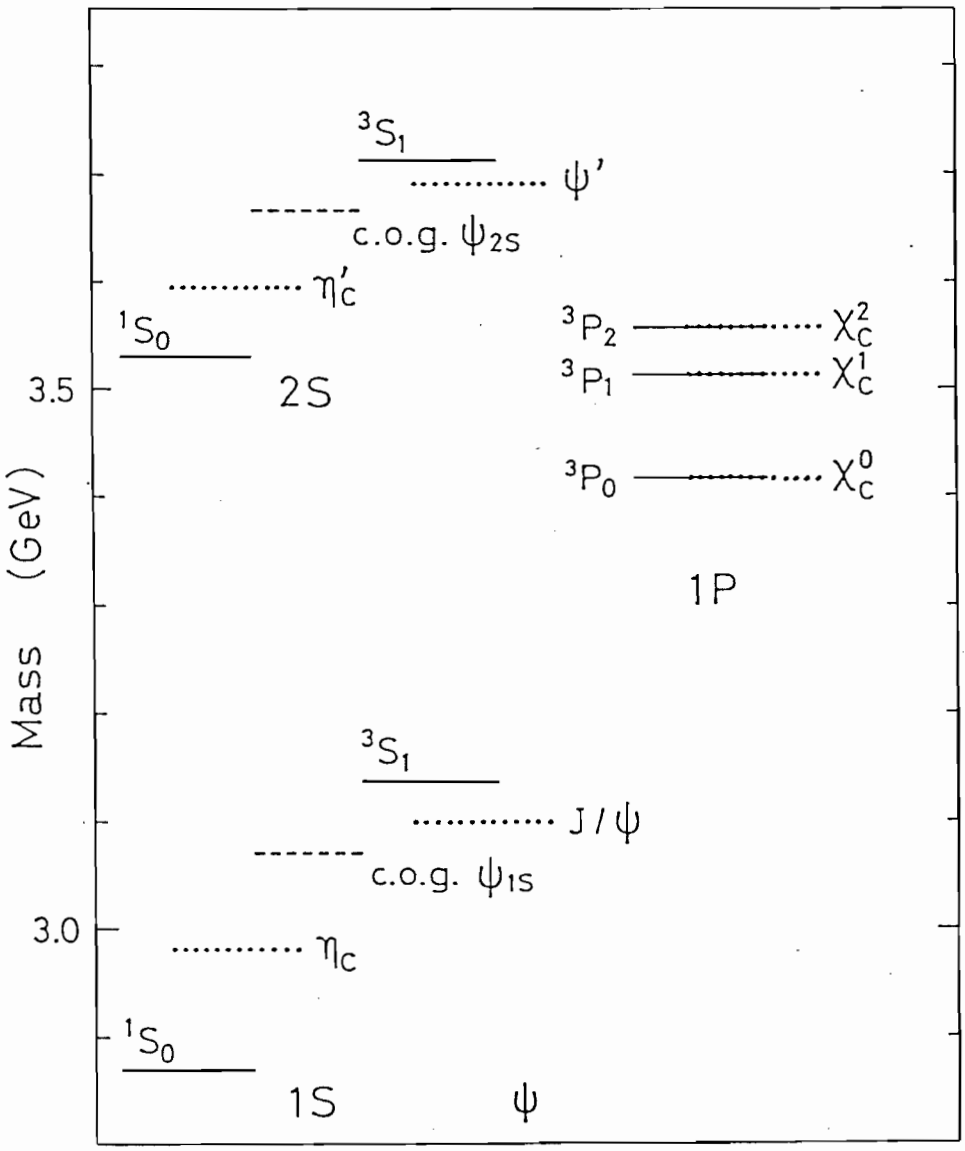

Fig. 1b. Spectra in the linear plus Coulomb model which reproduces the fine splitting of the 1P states for the chamonium. Parameters are a = 2.175 GeV^{-1}, b = −0.5752 GeV, α_s = 0.4706 and m_c = 1.183 GeV. The dotted lines are experimental data taken from reference (20). The dashed lines show the c.o.g. of $^3S_1$ and $^1S_0$.

4. MODIFICATION OF THE COULOMB POTENTIAL BY PERTURBATIVE QUANTUM CHROMODYNAMICS

As mentioned in the previous section, the hyperfine structure should be changed by an appropriate modification. This means that the vector potential should be corrected because the spin-spin term, eq.(2-7) is coming from the vector potential. We use the perturbative QCD in order to modifiy the short range part of the one gluon exchange potential. The modification of the potential at short distances may have a significant effect upon the fine and hyperfine structures since the spin dependent terms of the BF interaction have a relativistic origin and are sensitive to the short range behavior of the potential. Especially the hyperfine splitting is found to show more sensitivity from the short-range modification of the vector potential than the fine splitting does, as seen below. When the vector potential is written as

$$V(r) = -\frac{4}{3}\frac{\alpha_s(r)}{r}, \tag{4-1}$$

where $\alpha_s(r)$ is given by the two loop approximation as[12,13,21]

$$\begin{aligned}\alpha_s(r) = {} & \frac{12\pi}{33-2N_f}(\ln x^{-2})^{-1} \\ & \left[1+\left\{2\gamma_E + \frac{93-10N_f}{3(33-2N_f)}\right\}(\ln x^{-2})^{-1}\right. \\ & \left. - \frac{6(153-19N_f)}{(33-2N_f)^2}\ln(\ln x^{-2})(\ln x^{-2})^{-1}\right].\end{aligned} \tag{4-2}$$

Here $x = r\Lambda_{\overline{MS}}$, N_f is a number of flavors and γ_E is the Euler constant. The formula, eq.(4-2) is, however, to be used in the

small r region, say, $r \lesssim 0.3\ \mathrm{GeV}^{-1}$, which is estimated from the asymptotic free deep inelastic scattering. There are two ways to extend the potential, eq.(4-1) to large r region. One is from the idea of Richardson[13] and it is developed by Buchmüller and Tye.[12] Their potential has a single form and is chosen such that it coincides to the form eq.(4-1) at short distances and continuously connected to a linear confining potential. If one considers that the whole potential has a vector coupling to quark it is hopeless to reproduce the ^3P states of the charmonium, as mentioned in Section 3. Another difficulty in the vector confinement is that it cannot confine quarks according to the Klein paradox in the Dirac equation.[10,11] We think it undesirable that the region of their potential connected to the form of eq.(4-1) is $r < 0.05\ \mathrm{GeV}^{-1}$, since this region is too small to have any physical effects to the quarkonium spectra.

There is an alternative way which we adopt here. It is found that the potential in the intermediate region where the charmonium and bottomonium have their orbits ($r > 1\ \mathrm{GeV}^{-1}$) is well desribed by the linear plus Coulomb model. Therefore another way to extend the QCD potential, eq.(4-1) is to connect to the Coulomb form,

$$V(r) = -\frac{4}{3}\frac{\alpha_s^0}{r}, \quad (r > 1\ \mathrm{GeV}^{-1}) \tag{4-3}$$

where α_s^0 is a constant as the Coulombic coupling. We suppose that the scalar confining potential is given by eq.(3-2) again. For connecting eq.(4-1) to the above eq.(4-3) we introduce the vector potential as

$$V(r) = -\frac{4}{3}\frac{\alpha_s^0}{r}[1 - \exp\{-(\frac{r}{R_c})^{\sigma}\}], \tag{4-4}$$

with parameters α_s^0, R_c and σ, which are determined from the behavior of the QCD form, eq.(4-1) at short distances. It is noted that the potential form eq.(4-4) is easily treated in calculating H_{BF}, while the complicated form eq.(4-1) is too difficult. In eq.(4-4) $r = R_c$ is a turning point where V(r) changes from the QCD behavior of eq.(4-1) into the pure Coulomb form. In Figure 2 we illustrate the effects of eq.(4-4) to the fine and hyperfine splittings with appropriate parameters. It is found that the hyperfine splitting is very sensitive to the magnitude of the turning point R_c, which indicates the strength of modification but the fine splitting is not so sensitive as the hyperfine one. Thus we can expect desired results to remedy the difficulties we met in Section 3.

We take $R_c = 0.5\ \text{GeV}^{-1}$ in the present investigation so that the perturbative QCD form is reproduced in the asymptotic region.(See below.) Determination of the potential is rather insensitive to slight changes of R_c in the region $0.3\ \text{GeV}^{-1} - 0.6\ \text{GeV}^{-1}$. Because other parameters can be adjusted in order to reproduce the same results. Once R_c is fixed and $\Lambda_{\overline{MS}}$ is given, we can fit eq.(4-4) to eq.(4-1) in the region $0.1\ \text{GeV}^{-1} \leq r \leq 0.3\ \text{GeV}^{-1}$ and determine the parameters α_s^0 and σ uniquely. The region used in fitting is estimated from the asymptotic free region established by the deep inelastic scatterings. In eq.(4-2), we set $N_f = 4$ which is the effective number of flavors in the above r region. Because the average momentum transfer $\langle Q \rangle \simeq 1/\langle r \rangle$ in the topponium state is less than $2m_b$ as shown in Table 2 (See Section 5) and the present potential is defined to be independent of flavor. Figure 3 shows a potential given in Section 5 and one sees how well our connection of eq.(4-1) in the region $r < 0.3\ \text{GeV}^{-1}$ with the eq.(4.3) in $r > 1\ \text{GeV}^{-1}$ works. The form of eq.(4-4) gradually deviates from eq.(4-1) in the region $r \simeq 0.1$

GeV^{-1}, which is not so serious since this region is too small and does not give any physical effect to the heavy quarkonium spectra.

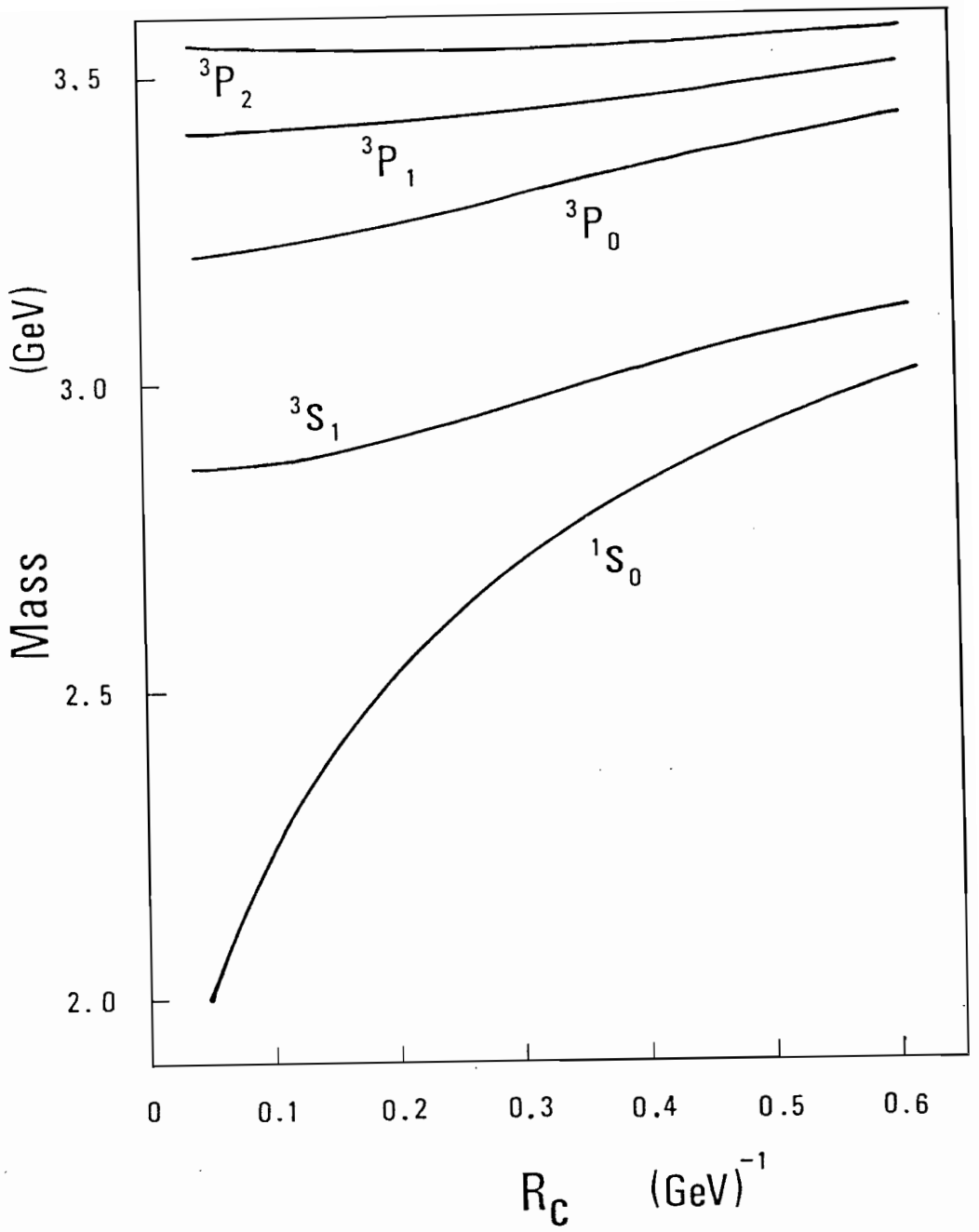

Fig. 2. Fine and Hyperfine splittings of $c\bar{c}$ 1S, 1P states as functions of R_c. By way of illustration parameters are chosen appropriately and we set $\sigma = 1$ for simplicity.

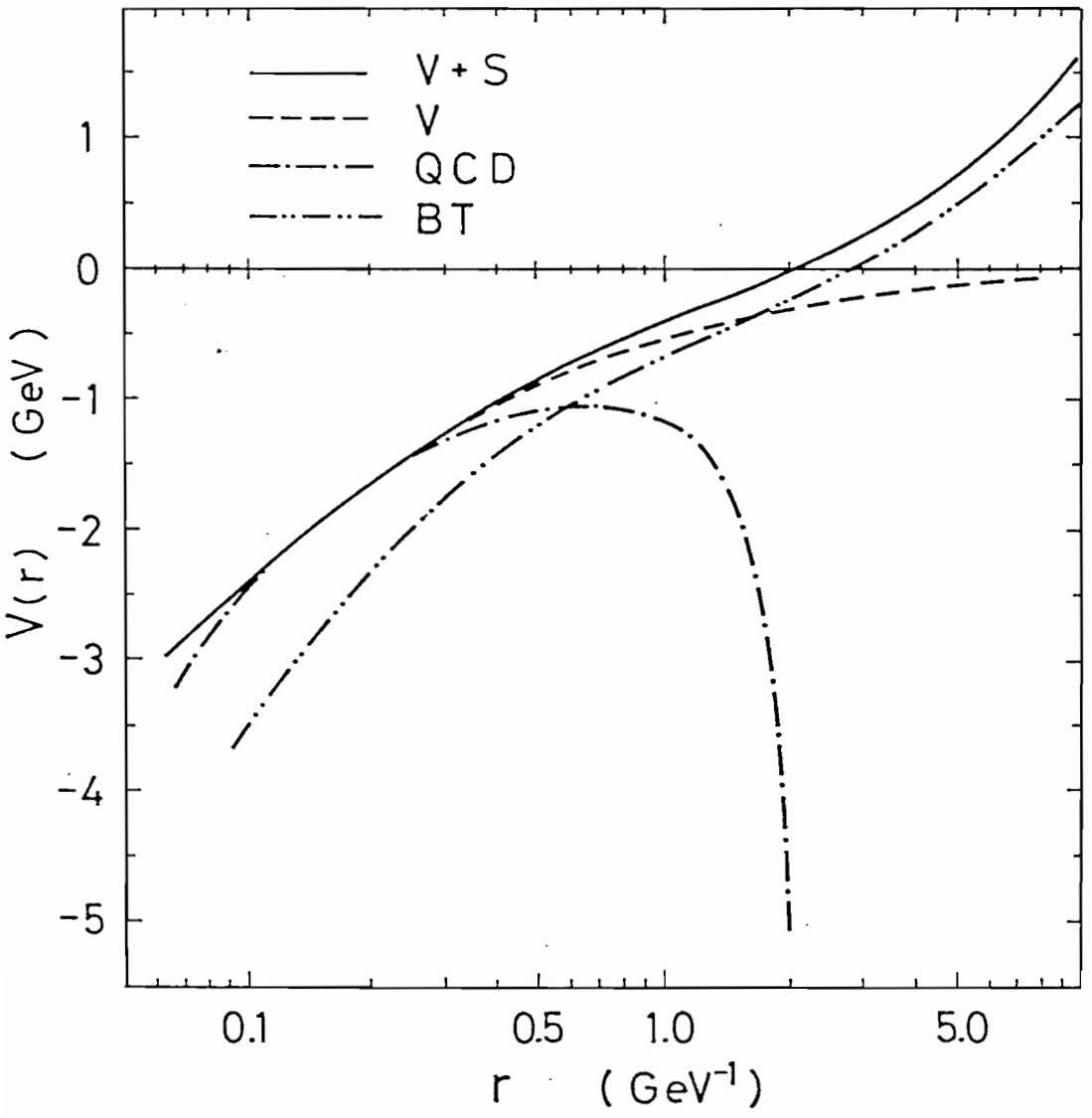

Fig. 3. The $Q\bar{Q}$ potential: the solid curve denote the whole potential, the vector V(r) plus scalar S(r). The dashed curve is the vector V(r) and the dash-dotted curve shows the perturbative QCD potential eq. (4-1). The dash-double-dotted curve corresponds to that of reference (12).

5. ENERGY LEVEL OF HEAVY QUARKONIA

5.1 Charmonium and Bottomonium

We examine effects of smearing the pure Coulomb potential around the origin according to perturbative QCD. As shown in Figure 2, the most significant effects is on the hyperfine splitting of the S states which are proportional to the probability at the origin in case of the pure Coulomb potential. On the other hand, the fine splittings of P and higher orbital angular momentum states are less affected by smearing since their orbit are farther from the origin than the S orbit. Fortunately the c.o.g.'s of the charmonium $c\bar{c}$ and the bottomonium $b\bar{b}$ are least affected by smearing at short distances. Conversely the situation is quite different in the topponium $t\bar{t}$ where the orbit becomes much smaller than that of the other heavy quarkonia and the top quark moves inside the smearing range independent of flavor. We will see in section 5.2 that even c.o.g.'s of the $t\bar{t}$ is strongly affected by perturbative QCD.

The best fit energy levels of $c\bar{c}$ and $b\bar{b}$ spectra are shown in Figure 3 and Table 1. We adopt the least square method to determine the potential parameters using the experimental values of the levels with asterisk in Figure 4 and Table 1 as input data and obtain

$$\Lambda_{\overline{MS}} = 0.36 \text{ GeV}, \quad a = 2.374 \text{ GeV}^{-1},$$
$$b = -0.030 \text{ GeV}, \quad m_c = 1.553 \text{ GeV}, \qquad (5\text{-}1)$$
$$m_b = 4.916 \text{ GeV},$$

and

$$R_c = 0.5 \text{ GeV}^{-1}, \quad \alpha_s^0 = 0.732,$$
$$\sigma = 0.582. \qquad (5\text{-}2)$$

Here parameters α_s^0 and σ of eq.(5-2) are obtained so as to fit

the perturbative QCD form of eq.(4-1) in the region $0.1\ \mathrm{GeV}^{-1} < r < 0.3\ \mathrm{GeV}^{-1}$ with R_c and $\Lambda_{\overline{MS}} = 0.36$. The calculated levels excellently agree with experiment. Consequently, this perturbative QCD tactics is successful. A little large α_s^0 plays a role to enlarge P state fine splittings as well in case of Figure 1b, while the smearing of the Coulomb potential aroud the origin reduces the hyperfine splittings of S states. We often refer to this potential as LCQCD which is abbriviation of the linear plus Coulomb potential modified by perturbative QCD.

The scale $\overline{MS}$ can be moved in the range $0.3\ \mathrm{GeV} < \Lambda_{\overline{MS}} < 0.4\ \mathrm{GeV}$, to give a nice fit to the experimental levels. On the contrary, in the range $\Lambda_{\overline{MS}} < 0.2$ GeV or $\Lambda_{\overline{MS}} > 0.5$ GeV it is difficult to find any parameter set to give a good fit to experiment. For example, if we choose $\Lambda_{\overline{MS}} = 0.2$ GeV, α_s^0 becomes too small to reproduce the experimental fine splitting in the charmonium 1P states. $\Lambda_{\overline{MS}}$ dependence of the $t\bar{t}$ states will be discussed in Section 5-2.

The potential with parameters of eqs.(5-1) and (5-2) is compared with that of Buchmüller and Tye (BT)[12] where its normalization is adjusted by shifting the potential with an appropriate constant. It is noted that there exists a significant gap between LCQCD and BT. The potential LCQCD differs from that of BT's by a constant in the outer region, $r > 0.5\ \mathrm{GeV}^{-1}$, while in the inner region, $r \lesssim 0.5\ \mathrm{GeV}^{-1}$, LCQCD potential has a more gentle slope than that of BT's does. The gap is explained as follows: First, the terms of eqs.(2-3), (2-6) and (2-12), T_{p4} and the spin independet interaction in the H_{BF} contribute to the shifts of c.o.g.'s. LCQCD potential is defined including these BF interactions and differs from that of BT's, which was fitted to ^3S states without the BF terms. Second point making this gap is that LCQCD at short distances

($r < 0.3\ \mathrm{GeV}^{-1}$) is well dominated by perturbative QCD. There, the confining potential almost vanishes compared with the vector part as shown in Figure 3. This indicates that we can take b = 0 in the confining potential since the linear term r/a^2 almost vanishes around the origin. $\Lambda_{\overline{MS}}$ dependence of b is given in Figure 5, which shows that b is small enough in the region $0.34\ \mathrm{GeV} < \Lambda_{\overline{MS}} < 0.37\ \mathrm{GeV}$. On the other hand, the BT potential has a nonperturbative tail in the asymptotic free domain and does not approach the perturbative form of eq.(4-1) until r becomes very small, say, $r \lesssim 0.05\ \mathrm{GeV}^{-1}$. This nonperturbative effects in the asymptotic free domain may bring forth a problem in the deep inelestic scatterings.

The $(p/m)^2$ expansion seems to work well when one looks over the ratio $\langle T_{p4} \rangle / \langle T \rangle$ in Table 1. This expression may not be good in the higher excited states where the average momentum becomes large. The present calculations based on the linear confining potential seems to give larger masses systematically in the higher excited states such as 3S, 4S, 2P, 2D, etc. The c.o.g's of 2^3P in the $b\bar{b}$ states was recently observed as 10.249 GeV, which is estimated as 10.284 GeV in the present model. LCQCD predicts their largest fine splitting, $M(^3P_2)-M(^3P_0) = 40$ GeV. We however, need not be nervous about the shift because the effect of the continuum $B\bar{B}$ channel may not be negligible.

By the present potential, the hyperfine splitting of 1S states in the $b\bar{b}$ is predicted as 66 MeV, which is almost a half of that in the naive linear plus Coulomb potential.[3] The experiment to search the singlet partner of Υ, would be a rigorous test for the hyperfine structure of the heavy quarkonium. Contrary to the Coulomb potential, the present vector potential causes hyperfine splittings not only to the S states but also to all the states which have nonzero L, such as P

states. It is found, however, that these splittings are very small in the heavy quarkonia.

Table 1a

Energy levels and several expectation values of $c\bar{c}$ S, P, D states with the present potential (LCQCD). Energy levels with asterisk are used as input data in the parameter fitting. Parameters are given in eqs.(5-1) and (5-2). The spin-dependent expectation values are devided by the spin operator given in Table 5.

		1S	2S	3S	4S	5S
E	(GeV)	3.205	3.862	4.320	4.704	5.047
$\langle r \rangle$	(GeV^{-1})	1.803	3.711	5.255	6.602	7.697
$\langle (v_i/c)^2 \rangle$		0.246	0.304	0.373	0.439	0.520
$\lvert\Psi(0)\rvert^2$	(GeV^3)	0.075	0.048	0.041	0.038	0.036
$\langle T \rangle$	(GeV)	0.383	0.472	0.579	0.682	0.807
$\langle T_{p4} \rangle$	(GeV)	-0.053	-0.083	-0.119	-0.158	-0.210
$\langle V \rangle$	(GeV)	-0.573	-0.345	-0.267	-0.225	-0.201
$\langle V_{SI} \rangle$	(GeV)	-0.051	-0.107	-0.128	-0.140	-0.157
$\langle S \rangle$	(GeV)	0.290	0.628	0.902	1.141	1.336
$\langle S_{SI} \rangle$	(GeV)	-0.024	-0.011	-0.007	-0.004	-0.001
$\langle V_{SS} \rangle$	(GeV)	0.034	0.020	0.016	0.014	0.013
$^3L_{L+1}$	(GeV)	3.112*	3.679*	4.084	4.416	4.691
^1L_L	(GeV)	2.975*	3.600*	4.019	4.359	4.640

Table 1a

(continued)

		1P	2P	3P	4P
E	(GeV)	3.669	4.156	4.556	4.908
$\langle r \rangle$	(GeV^{-1})	2.968	4.609	6.017	7.279
$\langle (v_i/c)^2 \rangle$		0.266	0.338	0.406	0.471
$\lvert\Psi(0)\rvert^2$	(GeV^3)				
$\langle T \rangle$	(GeV)	0.413	0.524	0.631	0.732
$\langle T_{p4} \rangle$	(GeV)	-0.043	-0.083	-0.123	-0.166
$\langle V \rangle$	(GeV)	-0.346	-0.262	-0.218	-0.191
$\langle V_{SI} \rangle$	(GeV)	-0.073	-0.103	-0.119	-0.131
$\langle S \rangle$	(GeV)	0.497	0.788	1.038	1.262
$\langle S_{SI} \rangle$	(GeV)	-0.039	-0.027	-0.021	-0.017
$\langle V_{SS} \rangle$	(GeV)	1.9×10^{-3}	1.6×10^{-3}	1.5×10^{-3}	1.4×10^{-3}
$\langle V_{LS} \rangle$	(GeV)	0.047	0.038	0.033	0.031
$\langle S_{LS} \rangle$	(GeV)	-0.014	-0.011	-0.009	-0.008
$\langle V_T \rangle$	(GeV)	7.0×10^{-3}	5.5×10^{-3}	4.8×10^{-3}	4.4×10^{-3}
$^3L_{L+1}$	(GeV)	3.545*	3.970	4.316	4.617
^3L_L	(GeV)	3.496*	3.929	4.279	4.581
$^3L_{L-1}$	(GeV)	3.421*	3.869	4.226	4.532
^1L_L	(GeV)	3.508	3.939	4.288	4.590

Table 1a

(continued)

		1D	2D	3D
E	(GeV)	3.987	4.404	4.767
$\langle r \rangle$	(GeV^{-1})	3.956	5.426	6.733
$\langle (v_i/c)^2 \rangle$		0.302	0.373	0.440
$\lvert\Psi(0)\rvert^2$	(GeV^3)			
$\langle T \rangle$	(GeV)	0.468	0.579	0.683
$\langle T_{p4} \rangle$	(GeV)	-0.049	-0.090	-0.133
$\langle V \rangle$	(GeV)	-0.258	-0.213	-0.186
$\langle V_{SI} \rangle$	(GeV)	-0.056	-0.080	-0.096
$\langle S \rangle$	(GeV)	0.672	0.933	1.165
$\langle S_{SI} \rangle$	(GeV)	-0.068	-0.054	-0.045
$\langle V_{SS} \rangle$	(GeV)	0.5×10^{-3}	0.5×10^{-3}	0.4×10^{-3}
$\langle V_{LS} \rangle$	(GeV)	0.016	0.014	0.013
$\langle S_{LS} \rangle$	(GeV)	-0.010	-0.009	-0.007
$\langle V_T \rangle$	(GeV)	2.4×10^{-3}	2.1×10^{-3}	1.9×10^{-3}
$^3L_{L+1}$	(GeV)	3.825	4.190	4.504
^3L_L	(GeV)	3.815	4.179	4.492
$^3L_{L-1}$	(GeV)	3.790	4.155	4.468
^1L_L	(GeV)	3.814	4.179	4.492

Table 1b

Energy levels and several expectation values of $b\bar{b}$ S, P, D states. Notations are the same as Table 1a.

		1S	2S	3S	4S	5S
E	(GeV)	9.485	10.093	10.461	10.752	11.012
$\langle r \rangle$	(GeV^{-1})	0.994	2.257	3.331	4.263	4.802
$\langle (v_i/c)^2 \rangle$		0.082	0.081	0.092	0.104	0.133
$\lvert\psi(0)\rvert^2$	(GeV^3)	0.499	0.250	0.193	0.167	0.161
$\langle T \rangle$	(GeV)	0.404	0.399	0.451	0.513	0.655
$\langle T_{p4} \rangle$	(GeV)	-0.020	-0.022	-0.027	-0.033	-0.047
$\langle V \rangle$	(GeV)	-0.898	-0.509	-0.384	-0.320	-0.297
$\langle V_{SI} \rangle$	(GeV)	-0.028	-0.046	-0.049	-0.052	-0.063
$\langle S \rangle$	(GeV)	0.146	0.370	0.561	0.726	0.822
$\langle S_{SI} \rangle$	(GeV)	-3.9×10^{-3}	-1.4×10^{-3}	-5.2×10^{-3}	7.6×10^{-6}	5.5×10^{-4}
$\langle V_{SS} \rangle$	(GeV)	0.017	7.6×10^{-3}	5.6×10^{-3}	4.8×10^{-3}	4.3×10^{-3}
$^3L_{L+1}$	(GeV)	9.449*	10.030*	10.389	10.673	10.907
^1L_L	(GeV)	9.383	10.000	10.367	10.653	10.890

Table 1b

(continued)

		1P	2P	3P	4P
E	(GeV)	9.950	10.346	10.650	10.911
$\langle r \rangle$	(GeV^{-1})	1.767	2.899	3.878	4.731
$\langle (v_i/c)^2 \rangle$		0.075	0.085	0.098	0.111
$\lvert\Psi(0)\rvert^2$	(GeV^3)				
$\langle T \rangle$	(GeV)	0.371	0.420	0.480	0.547
$\langle T_{p4} \rangle$	(GeV)	-0.012	-0.018	-0.025	-0.032
$\langle V \rangle$	(GeV)	-0.537	-0.390	-0.320	-0.278
$\langle V_{SI} \rangle$	(GeV)	-0.032	-0.040	-0.044	-0.047
$\langle S \rangle$	(GeV)	0.284	0.484	0.658	0.809
$\langle S_{SI} \rangle$	(GeV)	-6.2×10^{-3}	-3.9×10^{-3}	-2.7×10^{-3}	-2.0×10^{-3}
$\langle V_{SS} \rangle$	(GeV)	9.3×10^{-4}	6.8×10^{-4}	5.8×10^{-4}	5.3×10^{-4}
$\langle V_{LS} \rangle$	(GeV)	0.019	0.013	0.011	0.010
$\langle S_{LS} \rangle$	(GeV)	-2.7×10^{-3}	-1.7×10^{-3}	-1.4×10^{-3}	-1.2×10^{-3}
$\langle V_T \rangle$	(GeV)	2.7×10^{-3}	1.9×10^{-3}	1.4×10^{-3}	1.4×10^{-3}
$^3L_{L+1}$	(GeV)	9.917	10.295	10.589	10.839
^3L_L	(GeV)	9.890	10.276	10.573	10.825
$^3L_{L-1}$	(GeV)	9.857	10.253	10.554	10.808
^1L_L	(GeV)	9.897	10.282	10.577	10.829

Table 1b

(continued)

		1D	2D	3D
E	(GeV)	10.228	10.547	10.815
$\langle r \rangle$	(GeV^{-1})	2.454	3.476	4.384
$\langle (v_i/c)^2 \rangle$		0.078	0.091	0.104
$\lvert\Psi(0)\rvert^2$	(GeV^3)			
$\langle T \rangle$	(GeV)	0.386	0.447	0.509
$\langle T_{p4} \rangle$	(GeV)	-0.011	-0.018	-0.025
$\langle V \rangle$	(GeV)	-0.395	-0.319	-0.274
$\langle V_{SI} \rangle$	(GeV)	-0.022	-0.030	-0.034
$\langle S \rangle$	(GeV)	0.405	0.587	0.748
$\langle S_{SI} \rangle$	(GeV)	-0.010	-8.0×10^{-3}	-6.4×10^{-3}
$\langle V_{SS} \rangle$	(GeV)	2.3×10^{-4}	2.0×10^{-4}	1.8×10^{-4}
$\langle V_{LS} \rangle$	(GeV)	5.8×10^{-3}	4.8×10^{-3}	4.3×10^{-3}
$\langle S_{LS} \rangle$	(GeV)	-1.7×10^{-3}	-1.3×10^{-3}	-1.1×10^{-3}
$\langle V_T \rangle$	(GeV)	8.6×10^{-4}	7.0×10^{-4}	6.2×10^{-4}
$^3L_{L+1}$	(GeV)	10.193	10.498	10.756
^3L_L	(GeV)	10.183	10.490	10.748
$^3L_{L-1}$	(GeV)	10.167	10.476	10.737
^1L_L	(GeV)	10.184	10.491	10.750

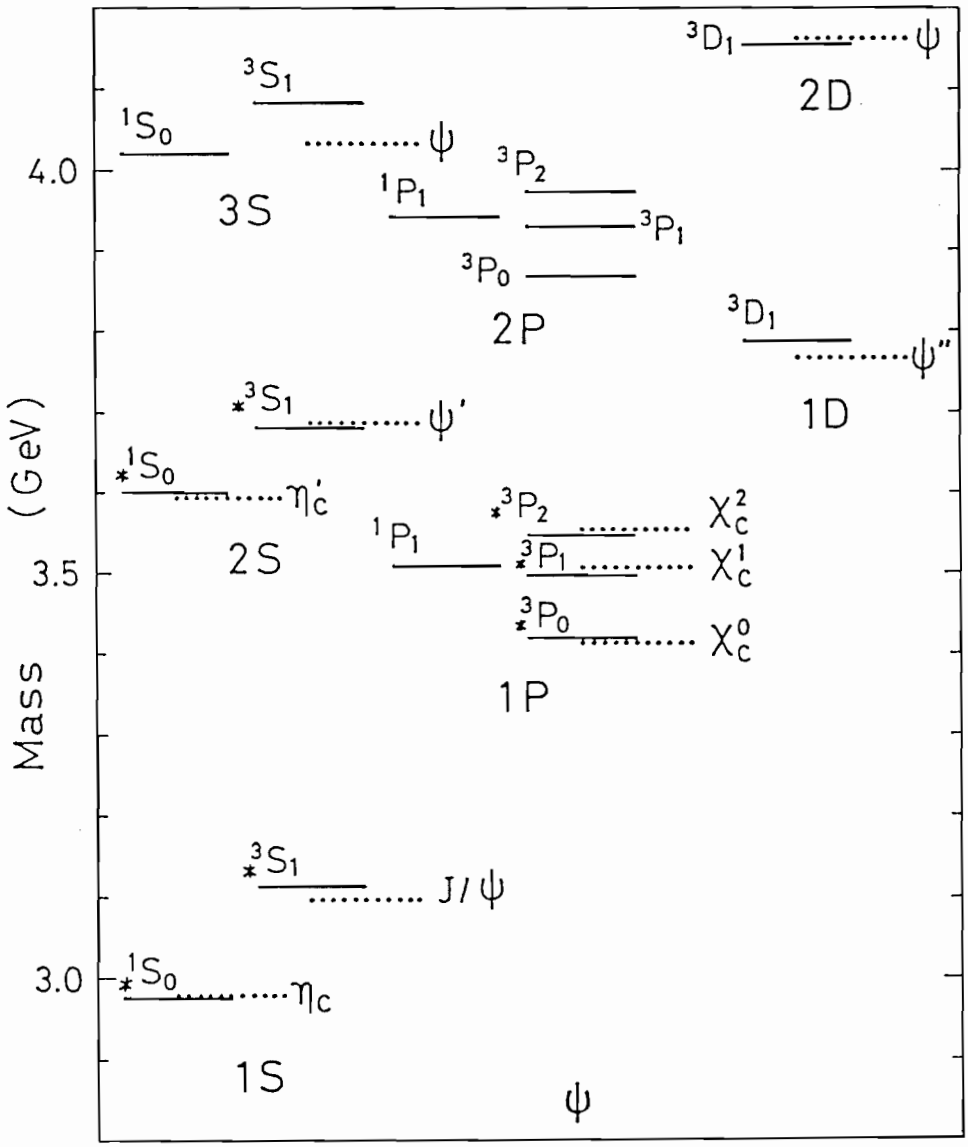

Fig. 4a. Calculated levels of $c\bar{c}$. The dotted lines are the experimental data taken from reference (20). The levels with asterisk are used as input data in the parameter fitting.

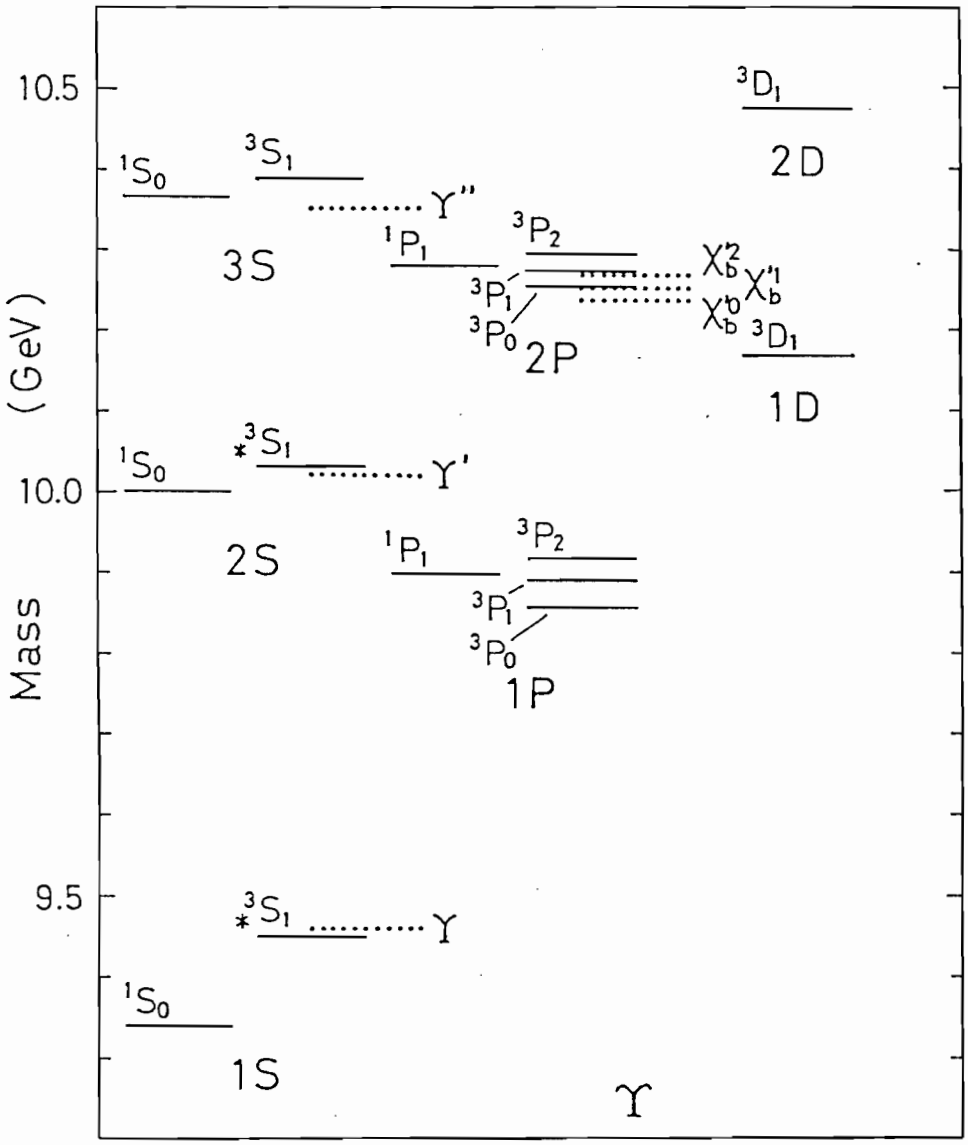

Fig. 4b. Calculated levels of $b\bar{b}$. Notations are the same as Figure 4a.

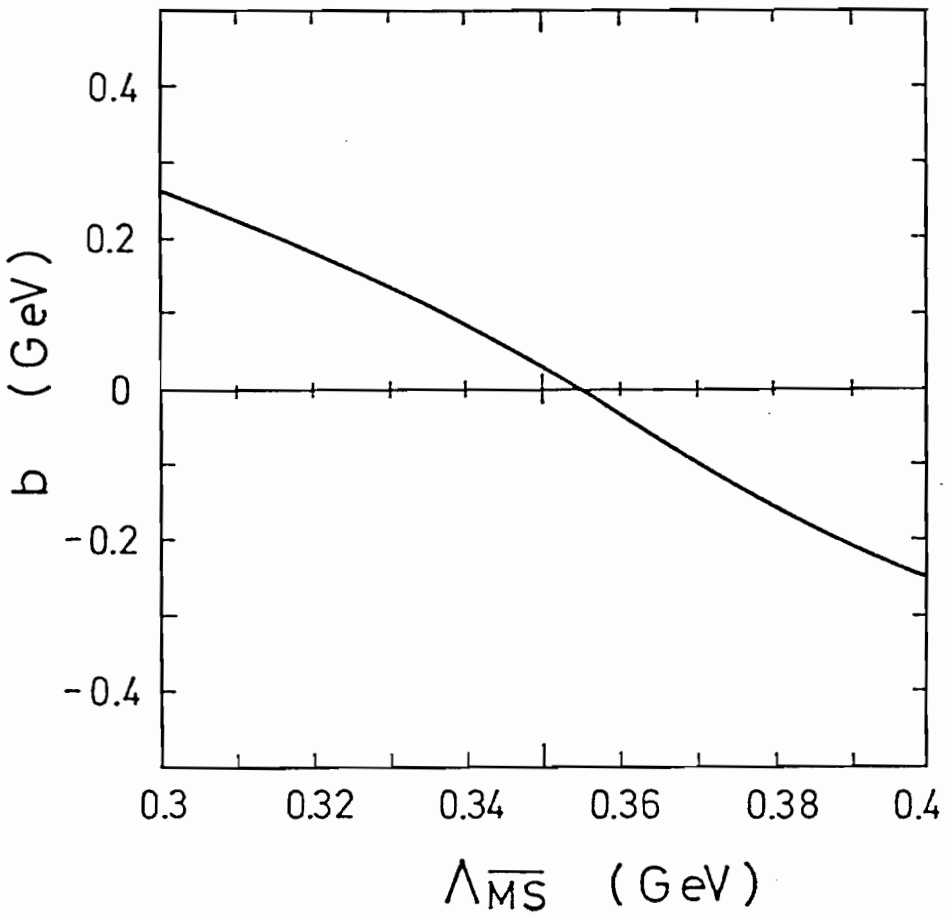

Fig. 5. $\Lambda_{\overline{MS}}$ dependence of b determined from the parameter fitting. Input data are the same as in Figure 4.

5.2 Topponium

Topponium spectroscopy is studied for several values of the top quark mass m_t in the expected range, 20 GeV $\leq m_t \leq$ 60 GeV with the LCQCD potential. Summaries of the results are given in Table 2 and in Figure 6. Even for the large top quark mass, the average orbit $\langle r \rangle$ of the ground state is not so small, $\langle r \rangle \simeq 0.2 - 0.5$ GeV^{-1}, compared with the case of naive linear plus Coulomb potential. This indicates that a top quark can not reach deep inside due to the QCD attenuation of the vector potential. Therefore, the ground state is pushed up and the level spacing becomes narrower, as shown in Figure 6a and 6b. The region of the top quark mass which experiments are expected is 30 GeV - 40 GeV. In this region the level spacing between 1S and 2S states is estimated about 800 MeV in LCQCD while in LC that becomes 1.3 GeV - 1.7 GeV. The hyperfine splittings of S states in the $t\bar{t}$ also become very small. At m_t = 30 GeV, for instance, $M(1^3S_1) - M(1^1S_0)$ = 27 MeV in the present potential, while it is about 500 MeV in the naive linear plus Coulomb potential (LC). For the P states, it is shown that spin-orbit force due to the scalar confining potential becomes negligible. We can expect the asymptotic form of the ratio eq.(3-1) as

$$R \sim \frac{2}{5} \frac{12 - 11\sigma - \sigma^2}{6 - 7\sigma + \sigma^2} = 0.93, \qquad (5\text{-}3)$$

for $m_t \to \infty$ and $\sigma = 0.582$ in LCQCD, Figure 7 shows the numerical results of the ratio R for the 1P and 2P states comparing LCQCD with LC. It is almost constant as $R \simeq 0.9$ in case of LCQCD and $R \simeq 0.8$ in case of LC. Thus studies of the level structure in the topponium afford a sensitive test of the potential form at short distances.

The scale $\Lambda_{\overline{MS}}$ in the perturbative QCD will also be

determined from the $t\bar{t}$ spectra. As the scale is raised from 0.3 GeV to 0.4 GeV, the vector potential around the origin becomes deep and binding energy of the $t\bar{t}$ system increases. The 1S binding energy in $\Lambda_{\overline{MS}} = 0.4$ GeV is 1.552 GeV at $m_t = 30$ GeV, which is compared with 0.765 GeV in $\Lambda_{\overline{MS}} = 0.3$ GeV. The level spacing between 1S and 2S is also larger by 60 MeV in $\Lambda_{\overline{MS}} = 0.4$ GeV than that in $\Lambda_{\overline{MS}} = 0.3$ GeV. $|\Psi(0)|^2$ has 5 % difference between them. Accordingly, the $t\bar{t}$ spectra will be sensitive enough to determine $\Lambda_{\overline{MS}}$.

Table 2

Energy levels and several expectation values of $t\bar{t}$ states versus top quark mass m_t.

	m_t	20	30	40	50	60
	1^1S_0	38.969	58.759	78.597	98.462	118.35
1S	1^3S_1	39.001	58.786	78.620	98.483	118.37
	$4\pi\|\Psi(0)\|^2$	77.618	164.18	280.20	424.69	596.93
	$\langle r \rangle$	0.439	0.343	0.288	0.251	0.224
	2^1S_0	39.676	59.517	79.398	99.301	119.22
2S	2^3S_1	39.687	59.526	79.406	99.308	119.23
	$4\pi\|\Psi(0)\|^2$	30.041	60.665	100.98	150.71	209.63
	$\langle r \rangle$	1.107	0.881	0.746	0.654	0.587
	3^1S_0	40.021	59.870	79.761	99.675	119.60
3S	3^3S_1	40.028	59.876	79.766	99.679	119.61
	$4\pi\|\Psi(0)\|^2$	19.582	37.722	60.934	89.074	122.03
	$\langle r \rangle$	1.757	1.428	1.224	1.083	0.978
	average	39.565	59.399	79.274	99.171	119.08
1P	$^3P_2-^3P_0$	0.027	0.021	0.018	0.017	0.02
	$\langle r \rangle$	0.844	0.668	0.563	0.493	0.442
	average	39.565	59.792	79.682	99.593	119.52
2P	$^3P_2-^3P_0$	0.015	0.011	0.010	0.009	0.01
	$\langle r \rangle$	1.508	1.220	1.043	0.921	0.830
1D	average	39.863	59.713	79.602	99.513	119.44
2D	average	40.132	59.983	79.877	99.793	119.72

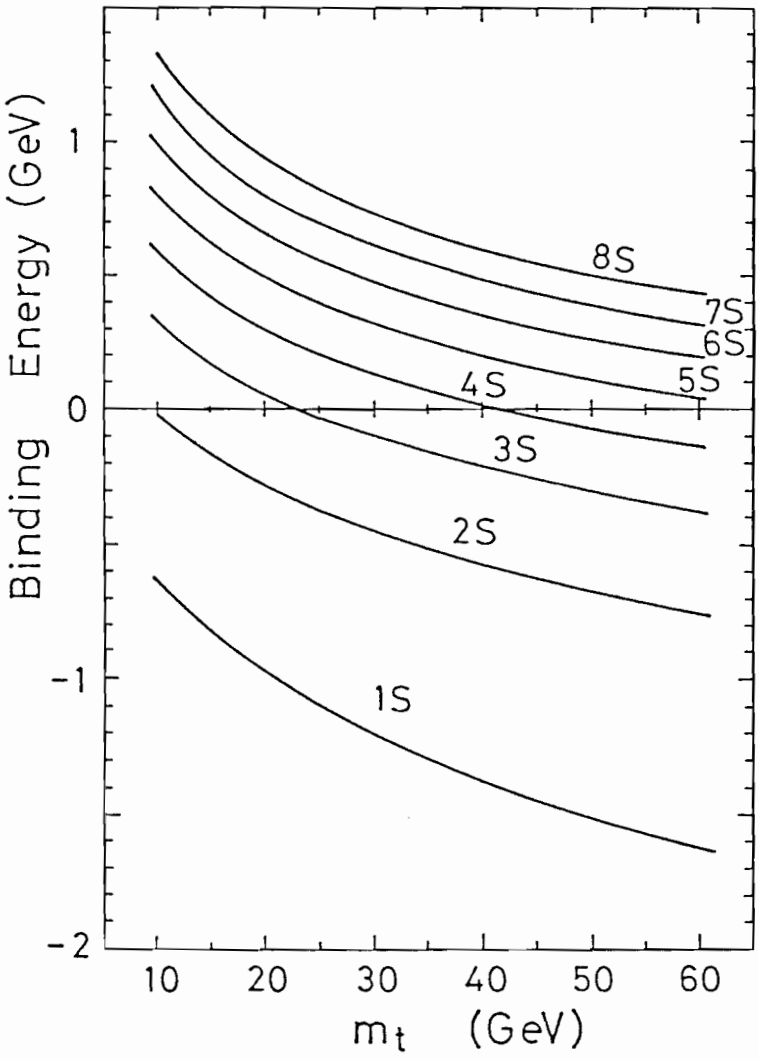

Fig. 6a. Top quark mass dependence of the c.o.g.'s of S states in the $t\bar{t}$ system in LCQCD.

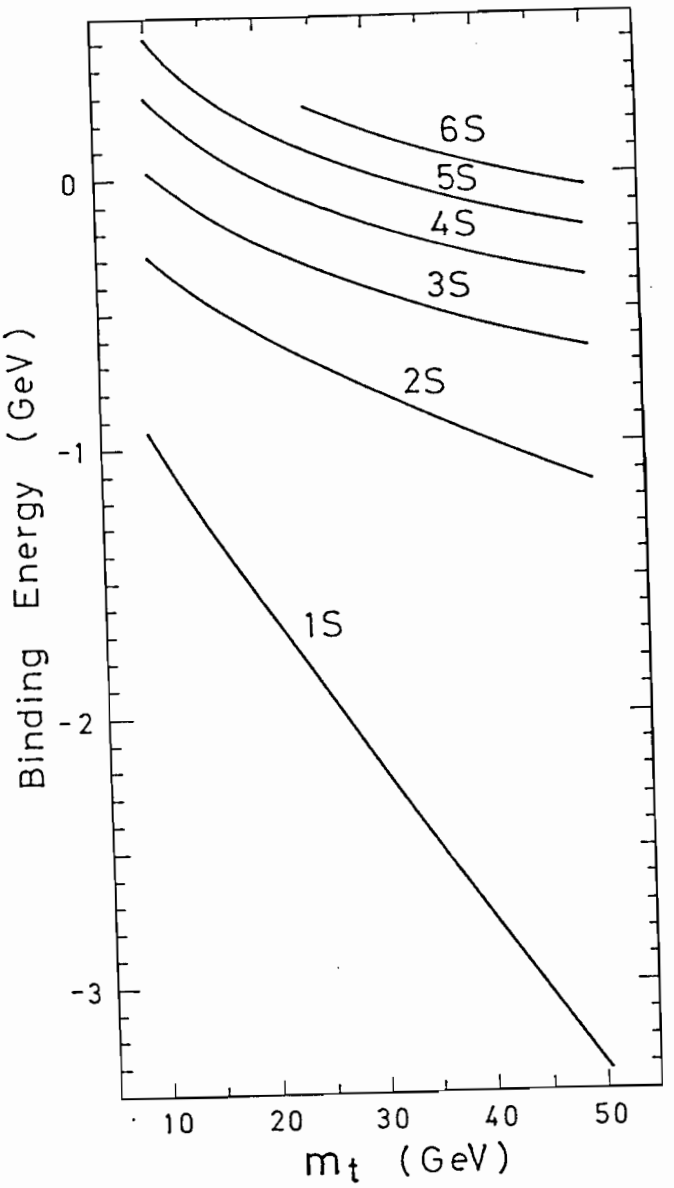

Fig. 6b. Top quark mass dependence of the c.o.g.'s of S states in the $t\bar{t}$ system in the linear plus Coulomb potential (LC). Parameters are the same as those in Figure 1a. It is found that the ground state energy is well described with the Bohr's semiclassical formula for the pure Coulomb potential.

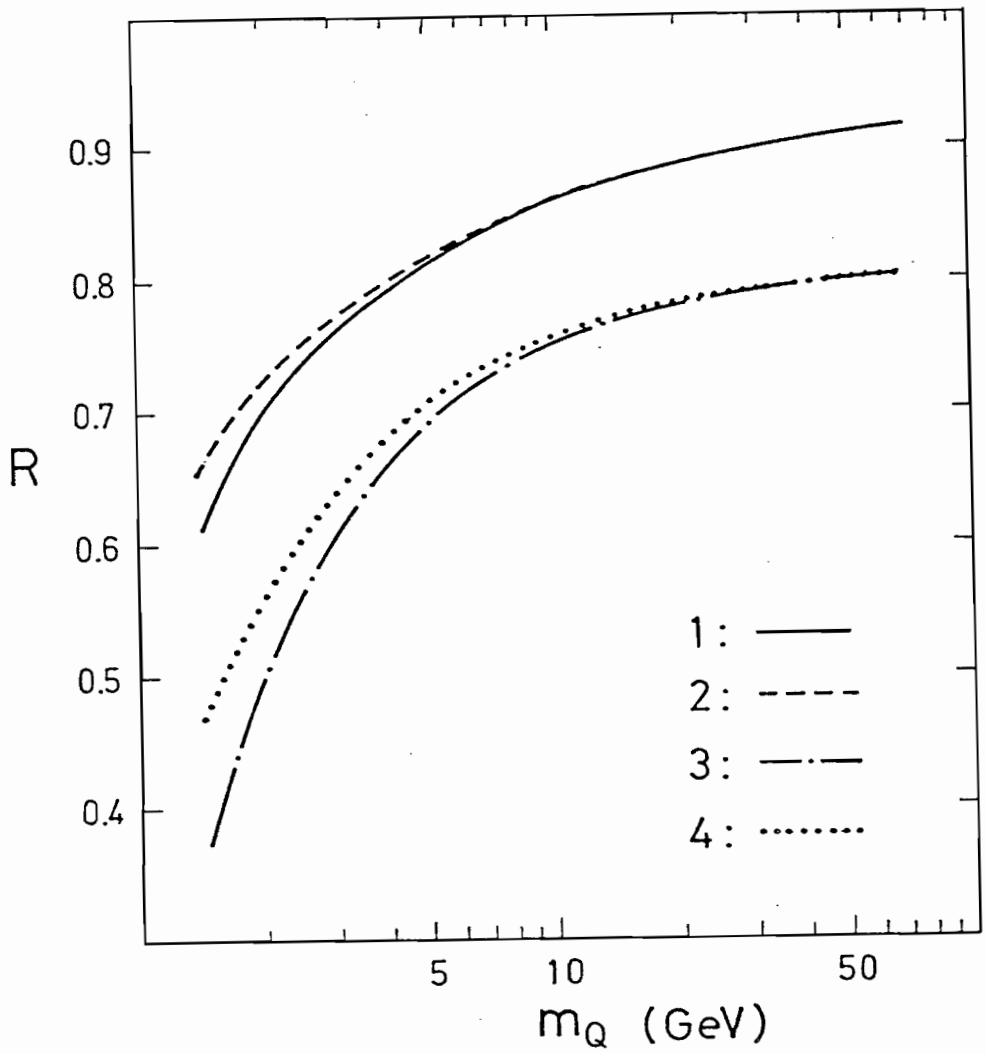

Fig. 7. Quark mass dependence of the ratio R, eq.(3-1) for LCQCD and LC. The numbers refer to, 1) 1P states (LCQCD), 2) 2P states (LCQCD), 3) 1P states (LC) and 4) 2P states (LC).

6. DECAYS OF HEAVY QUARKONIA

The smearing the vector potential by the perturbative QCD strongly affects the wave function at the origin which is closely related to the annihilation decay width of quarkonia. We use the annihilation decay formula with the first order QCD corrections given by Lepage et al.[21] There is a serious suspicion about apply this formula to the charmonium since the relativistic effect is not negligible. The decay formula factorized by $|\Psi(0)|^2$ will be well applied to the bottomonium since the relativistic effect is small ($(v/c)^2 \simeq 0.08$, see Table 1). The situation will be much better in the $t\bar{t}$ system. We determine $\tilde{\Lambda}_{\overline{MS}}$, independently of $|\Psi(0)|^2$, as $\tilde{\Lambda}_{\overline{MS}} = 115^{+30}_{-15}$ MeV from the experimental value of the muonic ratio of decay,

$$B_{\mu\mu}(\Upsilon) = \frac{\Gamma(\Upsilon \to \mu^+\mu^-)}{\Gamma(\Upsilon \to \text{all})} = 3.16 \pm 0.4. \qquad (6\text{-}1)$$

We can predict all the decay widths of heavy quarkonia by using the wave function at the origin, which has been evaluated in the previous section. The total anninilation widths of Υ, Υ', Υ'' and Υ''' are calculated in the present potential (LCQCD) and are compared with the linear plus Coulomb potential (LS)[3] and the power law potential (PL)[5]. The results are shown in Figure 8 and it is noted that LCQCD gives a good fit to the experiment of the total decay width of Υ, while LC gives too large and PL does rather small for it. It is hopeful to have the total annnihilation widths of the excited states in order to compare the predictions with experiment.

Decay widths of the $t\bar{t}$ ground state are shown in Figure 9 with $\tilde{\Lambda}_{\overline{MS}} = 0.115$ GeV. The formulas used in this section are

given in Appendix B. It is found that the total decay width slowly decreases as m_t increases up to $m_t \simeq 30$ GeV. This is strongly in contrast to LC, which predicts a sharp increase of the total decay width Γ_T. At $m_t = 30$ GeV, for instance, LCQCD gives $\Gamma_T = 45$ keV, while LC gives $\Gamma_T \simeq 400$ keV. Since the weak decay of type $t \to b+W$ does not depend upon the wave function at the origin, the branching ratio $B_W = \Gamma(t \to b+W)/\Gamma_T$ becomes large as m_t increases. At $m_t = 30$ GeV, $B_W = 22$ % in LCQCD, while $B_W \simeq 2 - 3$ % in LC.

The Drell ratio at the resonance peak is calculated by the formula

$$R_{peak} = \frac{9\pi}{2\alpha^2} \frac{\Gamma_h}{\Gamma_T} \frac{\Gamma_{ee}}{\Delta W} \times 0.4, \qquad (6\text{-}2)$$

when ΔW is the beam energy resolution and the factor 0.4 is just an estimate of the radiative crrections. Figure 10 shows R_{peak} for $\Delta W = 60$ MeV which gives $R_{peak} = 4$–5 for $m_t = 15$ to 40 GeV.

Radiative transition widths of the $c\bar{c}$ and $b\bar{b}$ are calculated and tabulated in Table 3. It is rather difficult to fit the cascade decay of the $c\bar{c}$ to experiment without considering the relativistic corrections.[23,24] For the M1 transition from $^3S_1$, to $^1S_0$, a calculation is also carried out with the relativistic correction and its results are presented, which agree fairly well with experiment. In the present paper farther detailed discussion is not made.

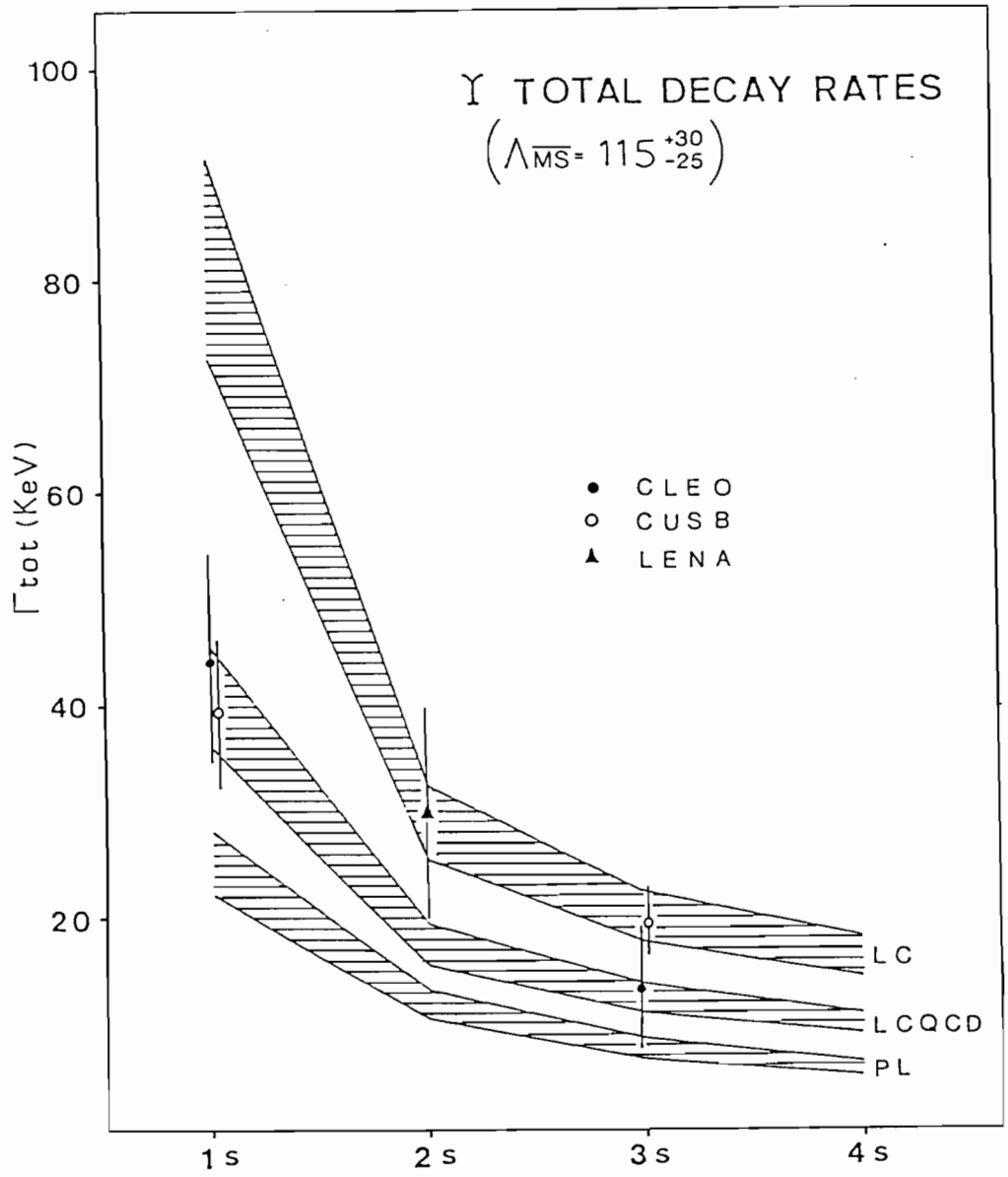

Fig. 8. Total annihilation widths of Υ, Υ', Υ'' and Υ''' for the present potential (LCQCD), for the linear plus Coulomb potential (LC)[3] and for the power law potential (PL).[5] Experimental data are taken from reference (22). It is noted that the data of the excited states include the non-annihilation contribution, for example, transition to lower $b\bar{b}$ states emitting photons or pions. The theoretical value must be compared with the one given by subtracting it from the raw data.

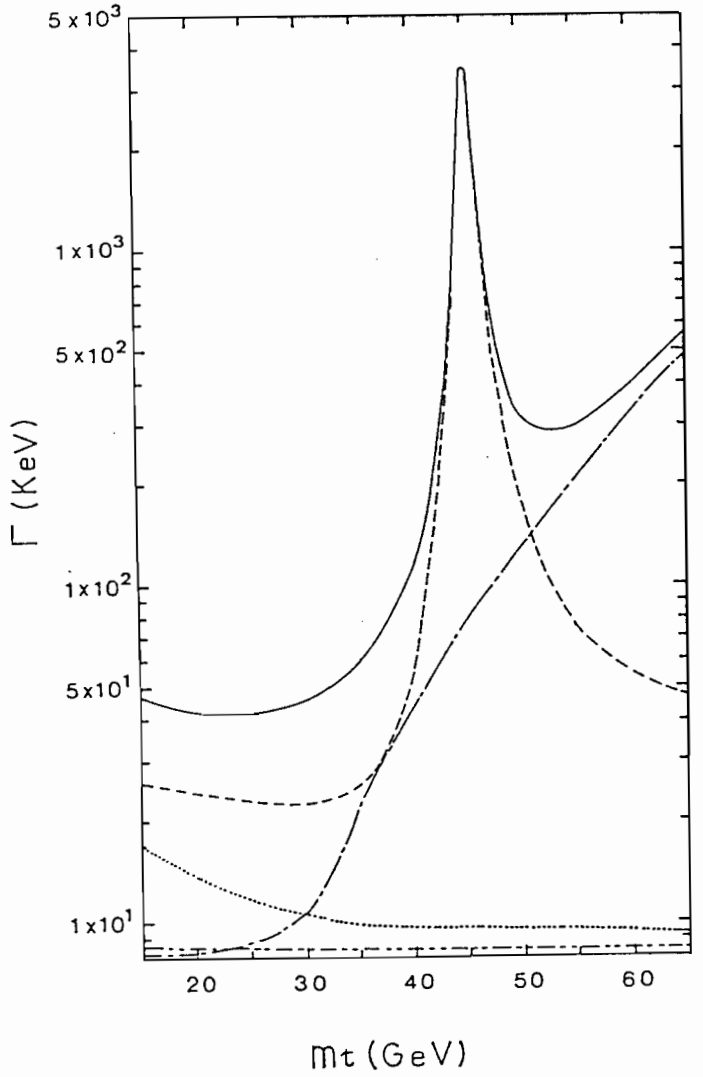

Fig. 9. Decay widths of the $t\bar{t}$ ground state: the solid curve denotes the accumurated total decay width, eq.(B-19). The dotted curve is the width $\Gamma(t\bar{t} \rightarrow 3g)$, eq.(B-2) and the dash-double-dotted curve shows $\Gamma(t\bar{t} \rightarrow \gamma 2g)$, eq.(B-3). The partial decay width $\Gamma(t\bar{t} \rightarrow \gamma^*, Z^* \rightarrow f\bar{f})$ in eq.(B-7) is given by the dashed curve. The dash-dotted curve is $\Gamma(t(\bar{t}) \rightarrow b(\bar{b})W)$ in eq.(B-5) due to the weak charged current. The sharp peak is due to the threshold of the Z boson. We take m_Z = 89 GeV and Γ_Z = 3 GeV.

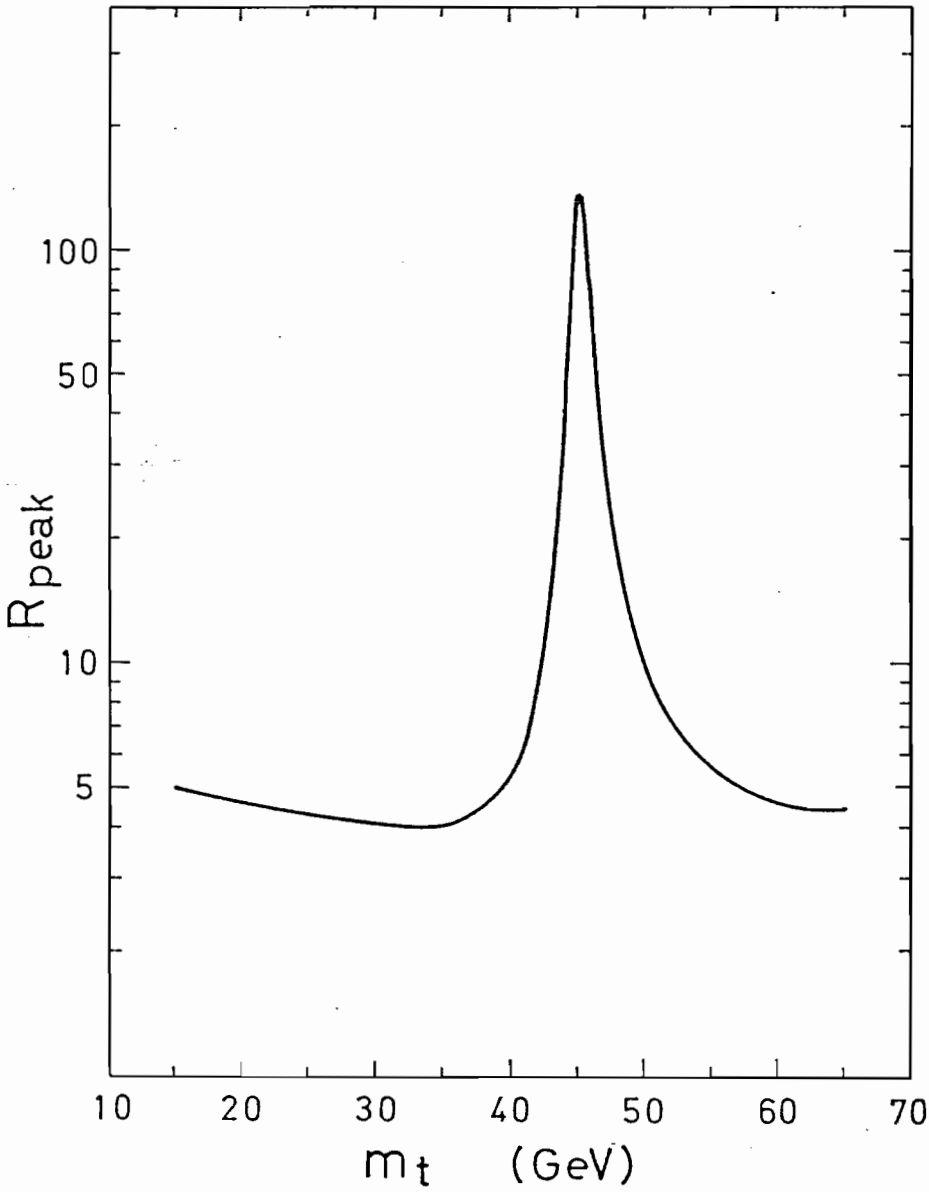

Fig. 10. Top quark mass dependence of R_{peak}. The sharp resonance-like peak at $m_t \simeq 45$ GeV is due to the Z boson production.

Table 3

Radiative decay widths (in keV) of $c\bar{c}$ and $b\bar{b}$ states. Results in parentheses are calculated with the relativistic correction terms according to reference (22).

transition	mode	$c\bar{c}$	$b\bar{b}$
	$1P(J=2) \rightarrow 1S$	535	40.2
	$(J=1)$	391	33.5
	$(J=0)$	178	26.3
	$2S \rightarrow 1P(J=2)$	33.5	1.6
	$(J=1)$	49.2	1.9
	$(J=0)$	59.3	1.2
	$3S \rightarrow 1P(J=2)$	-----	4.3×10^{-4}
	$(J=1)$	-----	3.1×10^{-4}
	$(J=0)$	-----	1.3×10^{-4}
E1			
	$2P(J=2) \rightarrow 1S$	-----	9.0
	$(J=1)$	-----	8.5
	$(J=0)$	-----	8.1
	$2P(J=2) \rightarrow 2S$	-----	18.7
	$(J=1)$	-----	15.5
	$(J=0)$	-----	12.6
	$3S \rightarrow 2P(J=2)$	-----	2.2
	$(J=1)$	-----	2.2
	$(J=0)$	-----	1.1

Table 3

(continued)

transition	mode	$c\bar{c}$	$b\bar{b}$
M1	$1^3S_1 \rightarrow 1^1S_0$	2.94	5.14×10^{-2}
		(1.19)	(4.28×10^{-2})
	$2^3S_1 \rightarrow 2^1S_0$	1.39	4.83×10^{-3}
		(0.21)	(3.66×10^{-3})
	$3^3S_1 \rightarrow 3^1S_0$	-----	1.91×10^{-3}
		-----	(1.30×10^{-3})

7. SUMMARY AND DISCUSSIONS

Heavy quark bound systems have been studied on the assumptions that [1] an asymptotic QCD form of the potential at short distances is continuously connected to the Coulomb potential and [2] a linear confining potential has a scalar coupling to a quark. The fine and hyperfine interactions are obtained from this potential by the FW transform. We think that a unified version of potential model for heavy quarkonium is established in this paper. The asymptotic QCD form of the potential plays an important role to reproduce the hyperfine splittings of the heavy quarkonia, and it has a large effect on the wave function at the origin, which gives a exellent fit to the Υ decays. It also has a direct influence on the topponium spectroscopy and decays.

There remains, however, some questions to be discussed. First, some objections to the Gromes' treatment[14] for the scalar retardation effect are made.[16,17] Miller and Olsson[16] suggest that the Gromes' treatment can not coincide the FW transform of the Dirac equation with the external field when one of two quarks has an infinite mass. We are suspicious that the equivalence between the BS equation and the Dirac equation in above limit may not hold when the retardation effects are taken into account. Barnes and Ghandour[17] raised objections not only to the treatment of Gromes' but also to that of Miller and Olsson's. They calculated the scattering amplitude for the scalar potential in the framework of $q_0 = 0$, zero energy transfer system. We think, however, that the retardation effects can not be appeared so as to work in the $q_0 = 0$ frame. Revealing this puzzle is left to future studies. Even if there exist some deviations from the present calculation, the conclusions of this

paper are not changed since the retardation effects from the scalar potential are several ten MeV in the charmonium and have effects on only c.o.g.'s of the heavy quarkonium spectra.

Another question is why the scale $\Lambda_{\overline{MS}}$ in the potential is different from the $\tilde{\Lambda}_{\overline{MS}}$ determined from the Υ decay. There are two kinds of terms which are not covered in the FW transform. One is the finite terms which appear in the perturvation of $O(\alpha_s^2(\mu))$ in the quark-antiquark scatterings. Another is singular terms proportional to $\ln(Q^2/m^2)$. The spin-spin interaction, for instance, is written as[7]

$$H_{ss} = \frac{8\pi}{3}\frac{\alpha_s(\mu)}{M^2}C_2(R)[1 + \frac{\alpha_s(\mu)}{\pi}K], \tag{7-1}$$

with

$$K = C + (7/8)C_2(G)\ln(Q^2/m^2) - (1/12)[11C_2(G)-4T(R)N_f]\ln(Q^2/\mu^2), \tag{7-2}$$

and

$$C = -(1/2)C_2(R) + (11/18)C_2(G) - (5/9)T(R)N_f + (16/9)C_2(R)(1-\ln 2), \tag{7-3}$$

where notations are also followed in reference (7). The first and second terms in eq.(7-2) are not covered in the FW transform but the third one is.

One possibility to implement the discrepancy between $\Lambda_{\overline{MS}}$ and $\tilde{\Lambda}_{\overline{MS}}$ is that the finite terms (C of eq.(7-3), for instance) play a role to adjust the scale. Although we know of the finite terms calculated by Gupta et al.[25] the exclusive calculations are open problem left to future studies. It is also noted that

there are some suggestions that the scale Λ may depend upon a certain process.[26] The singular term proportional to $\ln(Q^2/m^2)$ doubles the complexity.[6,25,27] A simple estimation shows that its contributions to the spin dependent terms in H_{BF} are not remarkable, as given in Table 4. Further theoretical studies are needed to estimate its numerical contribution.

Table 4a

Rough estiomation of the $\ln(Q^2/m^2)$ term (L) and the annihilation term (A) for the 1S hyperfine splittings.

1S	N_f	m_Q(GeV)	$\alpha_s(m_Q)$	L (MeV)	A (MeV)
$c\bar{c}$	3	1.553	0.478	22.54	1.45
$b\bar{b}$	4	4.916	0.288	2.61	0.35
$t\bar{t}$	5	20.0	0.204	- 0.14	0.13
		60.0	0.160	- 0.50	0.07

Table 4b

Rough estimation of the spin dependent $\ln(Q^2/m^2)$ terms for the 1P states. The LS and tensor terms are calculated according to the $\ln(Q^2/m^2)$ dependence in the vector coupling.[6,25]

1P	m_Q(GeV)	ΔV_{LS}(MeV)	ΔV_T (MeV)	ΔV_{SS}(MeV)
$c\bar{c}$	1.553	1.25	- 0.96	-12.65
$b\bar{b}$	4.916	- 1.45	- 0.58	- 3.15
$t\bar{t}$	20.0	- 0.89	- 0.28	- 1.16
	60.0	- 0.58	- 0.17	- 0.65

Appendix

A. Explicit Form of Operators Appeared in the BF Hamiltonian

In Section 2 the BF hamiltonian is obtained for a scalar and a vector potential. There appear several operators, which one may not be familiar with. In this appendix we specify their explicit form used in the present calculation.

Spin dependent operators are evaluated in Table 5 for given quantum numbers, L, S (total spin) and J, where only diagonal matrix elements are needed and shown so far as the first order perturbation.

Differential operators can be reduced those which act on w(r) in eq.(2-18). When there is an operator OV where O is a differential operator such as P^2 and V is a function of r. We define [O] as

$$\langle OV \rangle = \int (w^* [\ O\ ] w)(r) V(r) dr, \tag{A-1}$$

where O does not operate V. In this notation differential operators presented in Section 2 are written as

$$[\ p^2\ ] = -\vec{\partial}_r^2 + \frac{L(L+1)}{r^2}, \tag{A-2}$$

$$[\ p^4\ ] = \overleftarrow{\partial}_r^2 \cdot \vec{\partial}_r^2 - \frac{L(L+1)}{r^2}(\overleftarrow{\partial}_r^2 + \vec{\partial}_r^2) + \frac{L^2(L+1)^2}{r^4}, \tag{A-3}$$

$$[\ P^2\ ] = -\frac{1}{4}(\overleftarrow{\partial}_r^2 - 2\overleftarrow{\partial}_r \cdot \vec{\partial}_r + \vec{\partial}_r^2 + \frac{2}{r}(\overleftarrow{\partial}_r + \vec{\partial}_r) - \frac{4L(L+1)+2}{r^2}), \tag{A-4}$$

$$[\ (\vec{P}\cdot\vec{n})^2\ ] = -\frac{1}{4}(\overleftarrow{\partial}_r^2 - 2\overleftarrow{\partial}_r\cdot\vec{\partial}_r + \vec{\partial}_r^2 + -\frac{2}{r^2}). \qquad \text{(A-5)}$$

Here operators, $\vec{\partial}_r$ ($\overleftarrow{\partial}_r$) are d/dr which act on the initial (final) w(r) and not on the potential part V.

Table 5

Spin dependent operators in the H_{BF} for states which have orbital angular momentum L.

$^{2S+1}L_J$	$\vec{\sigma}_i \cdot \vec{L}$ (i=1,2)	$\vec{\sigma}_1 \cdot \vec{\sigma}_2$	S_{12}
$^3L_{L+1}$	L	1	$-\frac{2L}{2L+3}$
^1L_L	0	- 3	0
^3L_L	- 1	1	2
$^3L_{L-1}$	- 2L	1	$-\frac{2(L+1)}{2L-1}$

B. Decay formulas of the Heavy Quarkonium

Annihilation decay formulas are calculated with first order QCD correction by Lepage et al.[21] Partial widths of annihilation process, $\Gamma(Q\bar{Q} \rightarrow \mu\bar{\mu})$, $\Gamma(Q\bar{Q} \rightarrow 3g)$ and $\Gamma(Q\bar{Q} \rightarrow \gamma 2g)$ are written as,

$$\Gamma(Q\bar{Q} \rightarrow \mu\bar{\mu}) = \Gamma_{\mu\bar{\mu}} = 16\pi\alpha^2 e_Q^2 \frac{|\Psi(0)|^2}{M^2}\{1 - \frac{16}{3}\frac{\alpha_s(M^2)}{M^2}\}, \qquad (B\text{-}1)$$

$$\Gamma(Q\bar{Q} \rightarrow 3g) = \frac{160}{81}(\pi^2-9)\alpha_s^3(M^2)\frac{|\Psi(0)|^2}{M^2}\{1 + C\frac{\alpha_s(M^2)}{M^2}\}, \qquad (B\text{-}2)$$

and

$$\Gamma(Q\bar{Q} \rightarrow \gamma 2g) = \frac{128}{9}(\pi^2-9)\alpha e_Q^2 \alpha_s^2(M^2)\frac{|\Psi(0)|^2}{M^2} \times\{1 + C\frac{\alpha_s(M^2)}{M^2}\}. \qquad (B\text{-}3)$$

Here e_Q denotes a fraction of quark charge and M is a energy level of the $Q\bar{Q}$ system. $\alpha_s(Q^2)$ and C are defined by,

$$\alpha_s(Q^2) = \alpha_s^0[1 - \alpha_s^0(102-38N_f/3)/\{4\pi(11-2N_f/3)\} \times \ln\ln(Q^2/\Lambda^2)],$$

with

$$\alpha_s^0 = 4\pi/\{(11-2N_f/3)\ln(Q^2/\Lambda^2)\},$$

and

$$C = 4.95 \text{ for below } c\bar{c} \text{ threshold,}$$
$$= 3.80 \text{ for below } b\bar{b} \text{ threshold,}$$
$$= 3.10 \text{ for below } t\bar{t} \text{ threshold.}$$

In the heavy quarkonia weak decays also become important as well as those of annihilation, because weak decay width is proportional to m_Q^5. Partial widths of the weak process, $\Gamma(Q\bar{Q} \to W \to \text{all})$ and $\Gamma_W(t\bar{t} \to b\bar{b})$ are expressed as,

$$\Gamma(Q\bar{Q} \to W \to \text{hadron}) = 3x2xN_f G_\mu (m_Q/m_\mu)^5, \tag{B-4}$$

$$\Gamma(Q\bar{Q} \to W \to \text{all}) = 3x2xG_\mu (m_Q/m_\mu)^5 + \Gamma(Q\bar{Q} \to W \to \text{hadron}), \tag{B-5}$$

and

$$\Gamma_W(t\bar{t} \to b\bar{b}) = \{G_F^2/(3\pi)\}M^4 |\Psi(0)|^2/M^2. \tag{B-6}$$

Here $G_\mu = \Gamma(\mu \to e\nu\bar{\nu})$ and m_μ is the muon mass. G_F is the Fermi coupling constant.

In the topponium, weak neutral current has a significant effects on its decay width. From the standard Weinberg-Salam model, $\Gamma(t\bar{t} \to \gamma^*, Z^* \to \sum_f f\bar{f})$ is obtained as

$$\Gamma(t\bar{t} \to \gamma^*, Z^* \to \sum_f f\bar{f}) = \Gamma_{\mu\mu} \sum_f [e_f^2 + \frac{M^2}{\{(M^2-m_Z^2)^2+m_Z^2\Gamma_Z^2\}(2\sin 2\theta_W)^2}$$
$$\{2v_t v_f (e_f/e_t)(M^2-m_Z^2) + v_t^2(1+v_f^2)\frac{M^2}{e_t^2(2\sin 2\theta_W)^2}\}], \tag{B-7}$$

where f denotes a quark or a lepton. Here v_f is defined by

$$v_l = -1+4\sin^2\theta_W \text{ for } l = e, \mu, \tau,$$

$$v = 1,$$

$$v_q = 1-8/3\sin^2\theta_W \text{ for } q = u, c, t,$$

$$v_q = -1+4/3\sin^2\theta_W \text{ for } q = d, s, b.$$

M is the energy level of the $t\bar{t}$. We use $\sin^2\theta_W = 0.23$ and the mass and width of Z boson, $m_Z = 89$ GeV and $\Gamma_Z = 3$ GeV in the present calculation.

Consequently, the hadronic decay width Γ_{had} and the total decay width Γ_T of the $t\bar{t}$ ground state are given by,

$$\begin{aligned}\Gamma_{had} &= \Gamma(t\bar{t} \to 3g) + \Gamma(t\bar{t} \to \gamma 2g) \\ &+ \Gamma(t\bar{t} \to \gamma^*, Z^* \to \sum_q qq) \\ &+ \Gamma(t\bar{t} \to W \to \text{hadron}) + \Gamma_W(t\bar{t} \to b\bar{b}),\end{aligned} \tag{B-8}$$

and

$$\begin{aligned}\Gamma_T &= \Gamma(t\bar{t} \to 3g) + \Gamma(t\bar{t} \to \gamma 2g) \\ &+ \Gamma(t\bar{t} \to \gamma^*, Z^* \to \sum_f ff) \\ &+ \Gamma(t\bar{t} \to W \to \text{all}) + \Gamma_W(t\bar{t} \to b\bar{b}).\end{aligned} \tag{B-9}$$

REFERENCE

1) V. Barger, A.D. Martin and R.J.N.Phillips: Phys. Lett. 125B, 339 (1983);
R.M. Godbole, S. Pakvasa and D.P. Roy: Phys. Rev. Lett. 50, 1539 (1983).

2) VENUS Collaboration: Proposal TRISTAN-EXP-001 Jan, 1983;
TOPAS Collaboration: Proposal TRISTAN-EXP-002 Jan, 1983.

3) E. Eichten et al.: Phys. Rev. D17, 3090 (1978); E. Eichten et al.: Phys. Rev. D21,203 (1980).

4) C. Quigg and J.L. Rosner: Phys. Rep. C56, 168 (1979);
T. Appelquist et al.: Ann. Rev. Part. Sci. 38, 387 (1978);
S. Ono: Phys. Rev. D20, 2975 (1979).

5) A. Martin: Phys. Lett. 99B, 338 (1980).

6) H.J. Schnitzer: Phys. Rev. D19, 1566 (1979).

7) W. Buchmüller, Y.J. Ng and S.-H.H. Tye: Phys. Rev. D24,3003 (1981).

8) W. Buchmüller: Phys. Lett. 112B, 479 (1982);
S. Ono and F. Schöberl: Phys. Lett. 118B, 419 (1982);
H. Ito: Contribution paper to XXI Int. Conf. on High Energy Phys., Paris July 1982;
M. Hirano et al.: Prog. Theor. Phys. 67, 1251 (1982);
T. Murota: preprint Yamanashi 82-01, May 1982.

9) H.J. Schnitzer: Phys. Rev. Lett. 35, 1540 (1975);
A.B. Henriques et al.: Phys. Lett. 64B, 85 (1976).

10) J.F. Gunion and L.F. Li: Phys. Rev. D12, 3583 (1975);
D.W. Dine: Nuovo Cimento 38A, 19 (1977).

11) M. Kaburagi et al.: Phys. Lett. 97B, 143 (1980);
M. Kaburagi et al.: Z. Phys. C - Particles and Fields 9, 213 (1981).

12) W. Buchmüller and S.-H.H. Tye: Phys. Rev. D24, 132 (1981).

13) J.L. Richardson: Phys. Lett. 82B, 272 (1979).

14) D. Gromes: Nucl. Phys. B131, 80 (1977).

15) A. DeRujula et al.: Phys. Rev. D12, 147 (1975).

16) K.J. Miller and M.G. Olsson: preprint MAD/PH/57 May 1982;
M.G. Ollson and K.J. Miller: Phys. Rev. D28,674 (1983).

17) T. Barnes and G.I. Ghandour: Phys. Lett. 118B, 411 (1982).

18) H.J. Schnitzer: Phys. Rev. Lett. 35, 1540 (1975); Phys. Rev. D13, 74 (1975); Phys. Lett. B65, 239 (1976).

19) L.-H. Chan Phys. Lett. B71, 422 (1977);
C.E. Carlson and F. Gross: Phys. Lett. B74, 404 (1978).

20) Particle Data Group: Review of Particle Properties LBL100, April 1982.

21) P.B. Mackenzie and G.P. Lepage: Phys. Rev. Lett. 47, 1244 (1981).

22) J. Lee-Franzini, talk at XXI Int. Conf. on High Energy Phys., Paris, July 1982. See also reference (20).

23) G. Feinberg and J. Sucher: Phys. Rev. Lett. 35, 1740 (1975);
J.S. Kang and J. Sucher: Phys. Rev. D18, 2698 (1978).

24) R. McClary and N. Byers: preprint UCLA/82/TEP/12;
G. Hardekopf and J. Sucher: preprint Maryland 82-043.

25) S.N. Gupta et al.: Phys. Rev. D26, 3305 (1982);
S.N. Gupta and S.F. Radford: Phys. Rev. D24, 2309 (1981);
ibid. D25, 3430 (1982).

26) H. Nakkagawa and A. Niegawa: preprint OCU-97, 1982; Phys. Lett. 119B, 415 (1982);
T.M. Stevenson: Phys. Rev. D23, 2916 (1981).

27) M. Dine: Phys. Lett. 81B, 339 (1979);
J.-M. Richard and D.P. Sidhu: Phys. Lett. 83B, 362 (1979);
G.P. Lepage: talk at the SLAC Summer Institute on Particle Physics, August 1981.